

Introduction to statistical shape analysis II: Semi- landmarks and beyond

Sara Rolfe

8/26/19



Outline

- How many landmarks are enough?
- Semi-landmarks
- Deformable Analysis
- Spherical Harmonic Representation



How many landmarks are enough to characterize shape and size variation?

- Criteria for landmarks to be homologous and reproducible results in very sparse data from images
- For many data sets, this may not be sufficient to capture shape changes, especially along curves or smooth surfaces
- Point-landmark too stringent for effective biometrics in many 3D applications

Watanabe, Akinobu. "How many landmarks are enough to characterize shape and size variation?." PloS one 13.6 (2018): e0198341.



How many landmarks are enough to characterize shape and size variation?

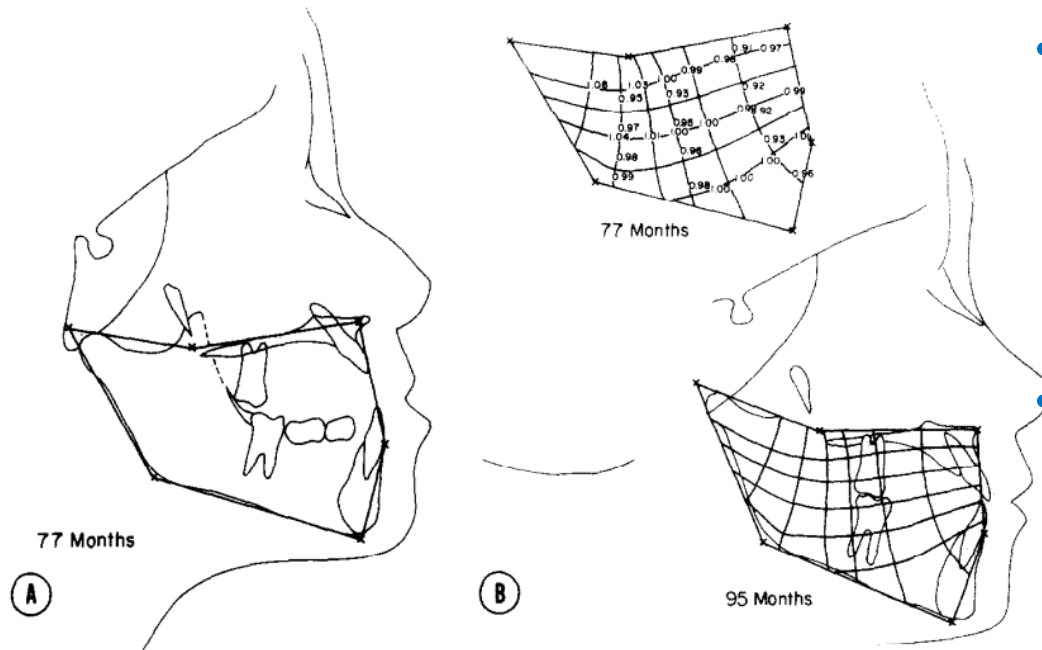
- Criteria for landmarks to be homologous and reproducible results in very sparse data from images
- For many data sets, this may not be sufficient to capture shape changes, especially along curves or smooth surfaces
- Point-landmark too stringent for effective biometrics in many 3D applications

Image data provides rich phenotype descriptions – how can this be leveraged?

Watanabe, Akinobu. "How many landmarks are enough to characterize shape and size variation?." PloS one 13.6 (2018): e0198341.



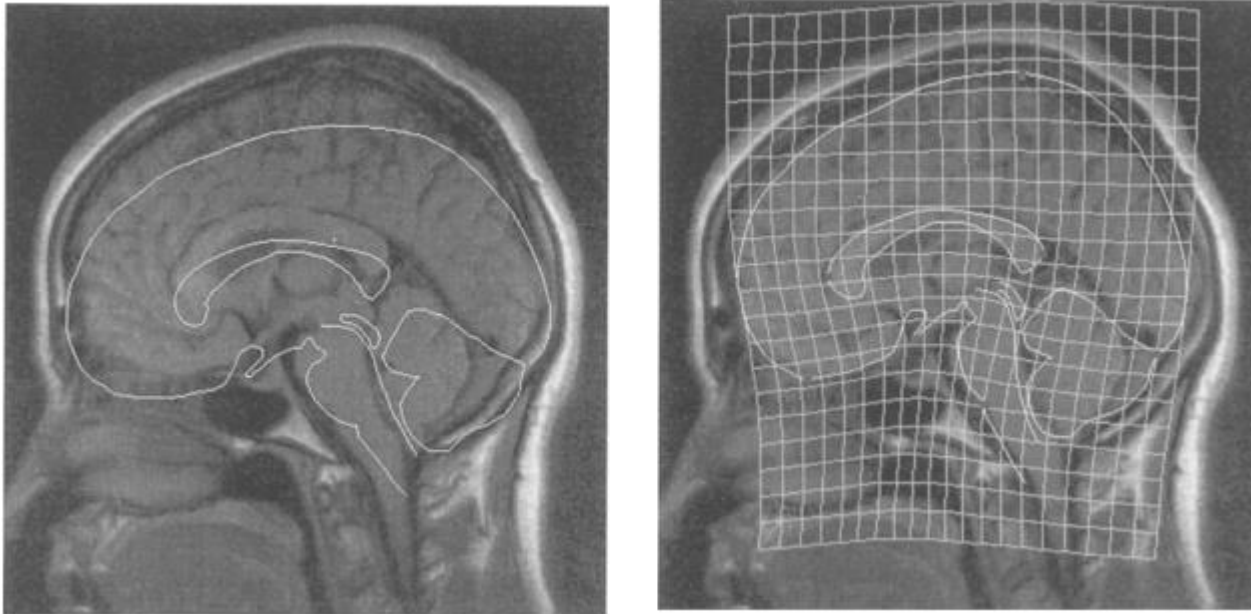
Constructed landmarks



- Geometric combinations of defined landmarks along lines erected at specific angles to define new landmarks
- Discarded since homology could not be fulfilled by these points

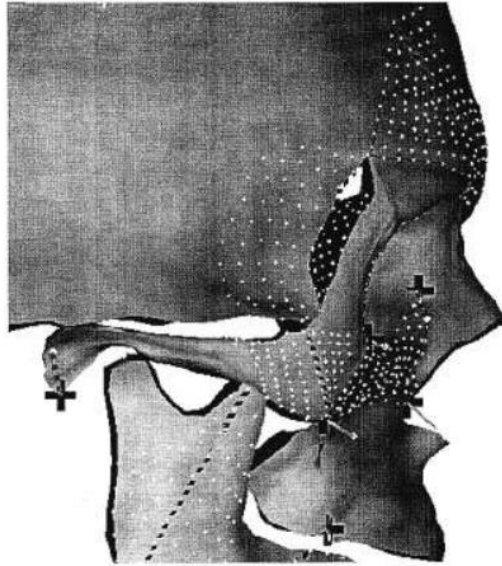
Moyers, Robert E., and Fred L. Bookstein. "The inappropriateness of conventional cephalometrics." *American Journal of Orthodontics and Dentofacial Orthopedics* 75.6 (1979): 599-617.

Extensions of TPS to include curvature



Bookstein, Fred L., and William DK Green. "A feature space for edgels in images with landmarks." *Journal of Mathematical imaging and vision* 3.3 (1993): 231-261.

Smooth surface analysis



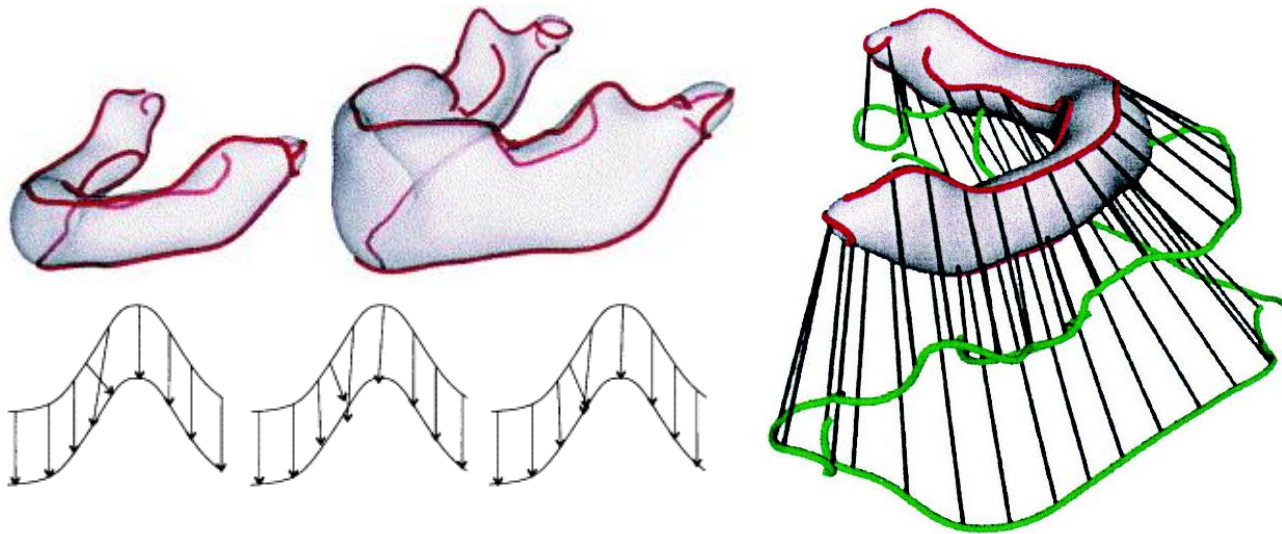
Combines the idea
of constructed
landmarks with
previous work on
parametric
averaging of
surfaces

- Thin-plate spline unwarping to the Procrustes mean configuration
- Equally spaced points are declared homologous along ridge curves and geodesics
- Evenly spaced points are declared homologous on the surface patches

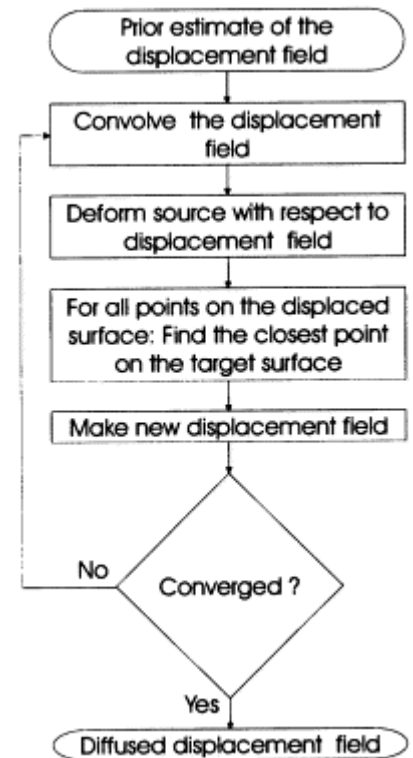
Cutting, Court, et al. "A three-dimensional smooth surface analysis of untreated Crouzon's syndrome in the adult." *The Journal of craniofacial surgery* 6.6 (1995): 444-453.



Geometry constrained diffusion



- Ridge lines, characterized by a minimax property of directional surface curvature, are extracted
- Curves are matched in order to establish object correspondence
- Correspondences subject to constraints

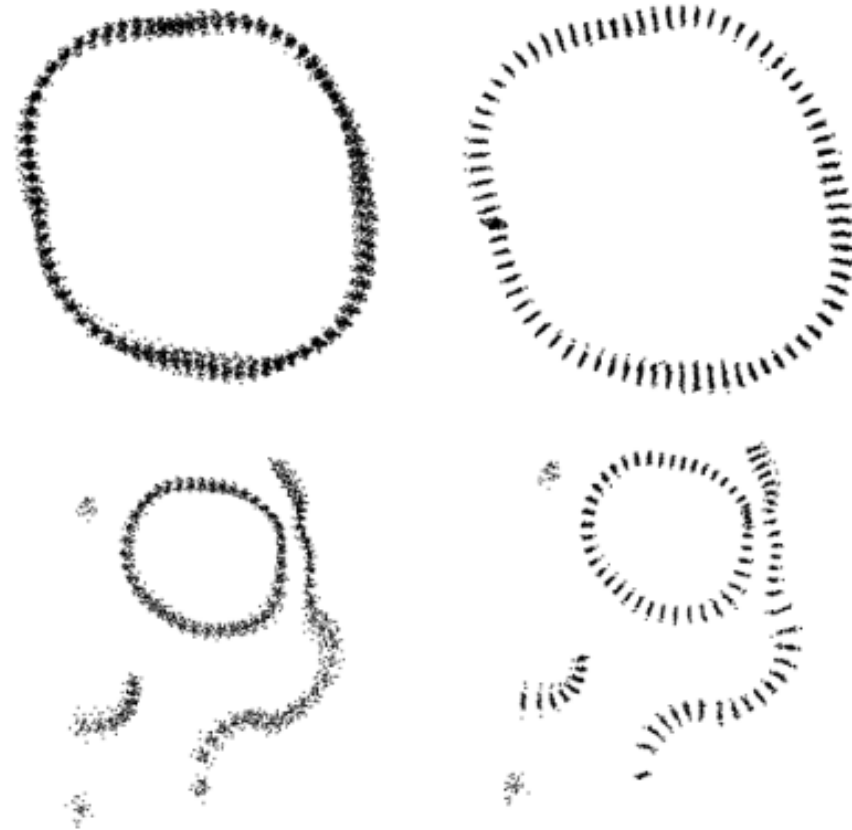


Andresen, Per Rønsholt, and Mads Nielsen. "Non-rigid registration by geometry-constrained diffusion." *Medical Image Analysis* 5.2 (2001): 81-88.



Sliding semi-landmarks

- Begin with structures that are known to correspond as parts (classical homology)
- Represents them by geometric curves or surfaces that generate reasonable mapping functions
- After Procrustes superimposition, semi-landmarks are slid along the surface to optimize correspondences



Before and after semi-landmark alignment of skull



What is wrong with equidistant samples?

Produce spacing as a by-product of the analysis since the analysis is ignorant of the actual spacing.



Figure 3. (a) Form with one true landmark in the lower left corner and 31 other points equally spaced along the outline. (b) Bent form with one true landmark (1) and 31 other points in equal spacing. (c) The position of the points now optimizes bending energy.

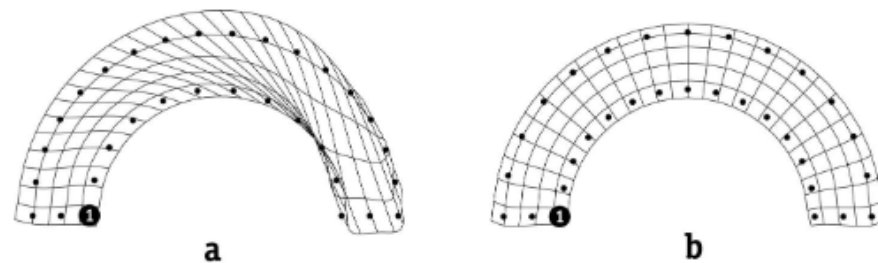
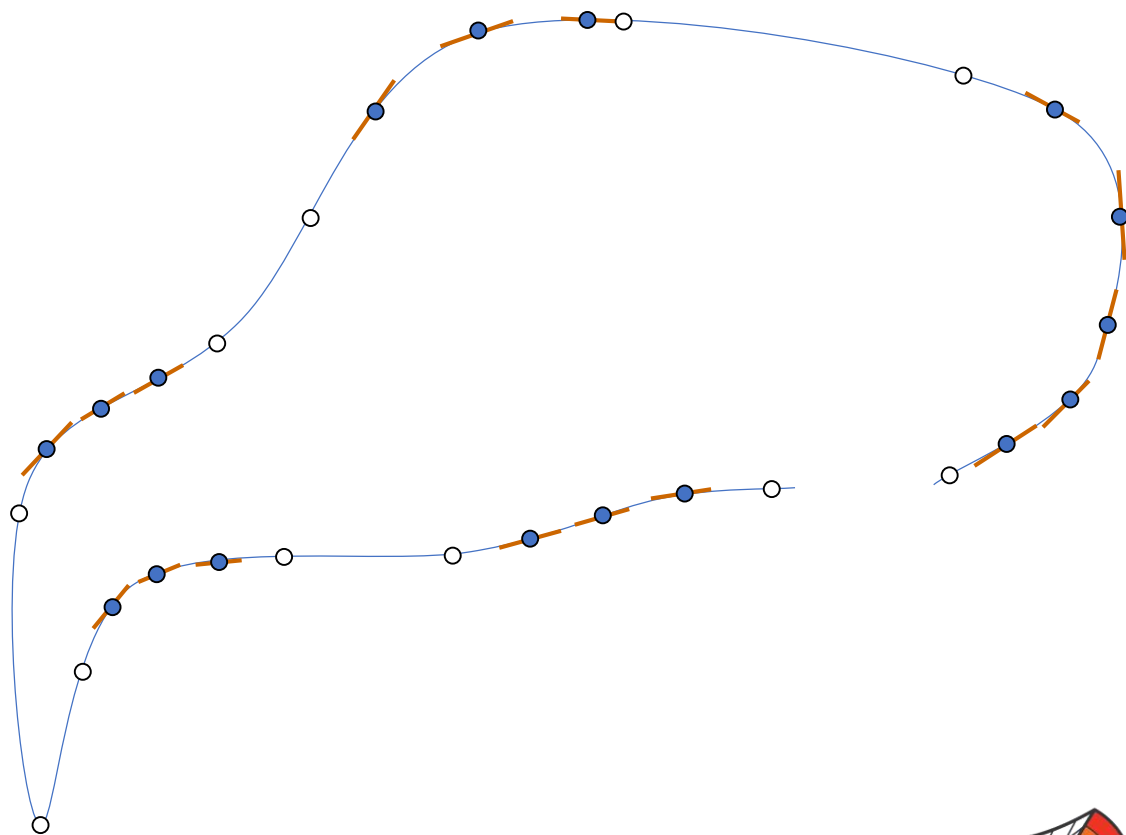


Figure 4. Splines corresponding to Figure 3. (a) Deformation grid from the form in Figures 3a and 3b. (b) Deformation grid from the form in Figures 3a and 3c.

Sliding semi-landmark method

- 1) Find optimal Procrustes alignment of samples using landmark points
- 2) Slide semi-landmark points along the surface until they satisfy matching criteria with a single reference specimen
- 3) Calculate Procrustes average shape
- 4) Slide semi-landmark points along the surface until they satisfy matching criteria with the Procrustes average
- 5) Repeat steps 3 and 4 until convergence



Bookstein, Fred L. "Landmark methods for forms without landmarks: morphometrics of group differences in outline shape." *Medical image analysis* 1.3 (1997): 225-243.

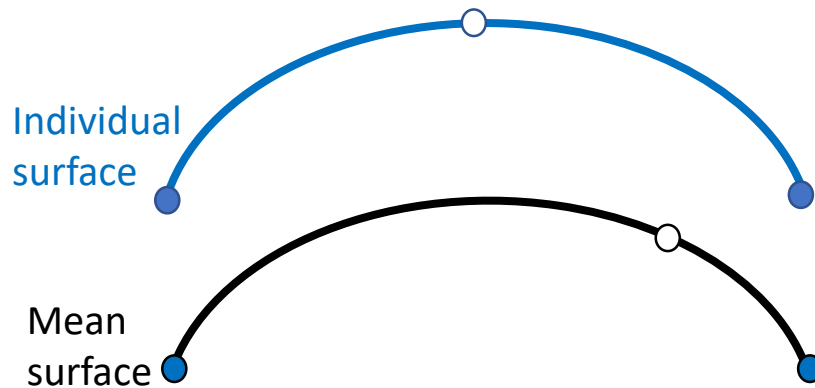


Determining position of sliding semi-landmarks

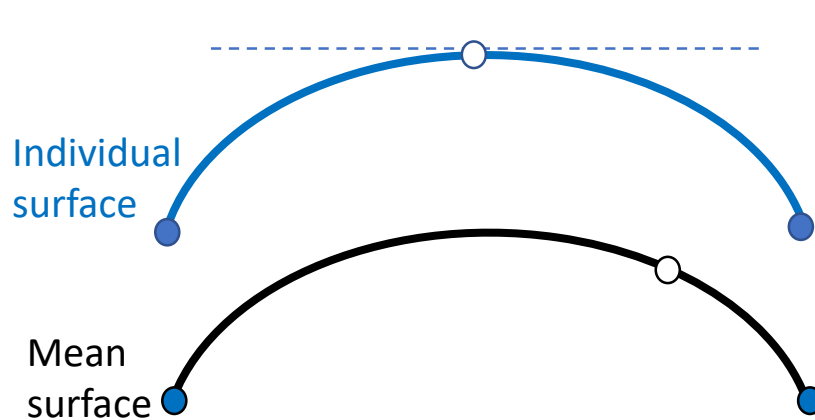
- 1) **Minimum bending energy criterion:** select semi-landmark positions that result in the smoothest possible transformation to the mean shape
- 2) **Procrustes distance criterion:** estimate the tangent to the mean surface for each semi-landmark point and remove the component of the difference between the mean and each specimen that lies along this tangent.



Minimum bending energy criteria

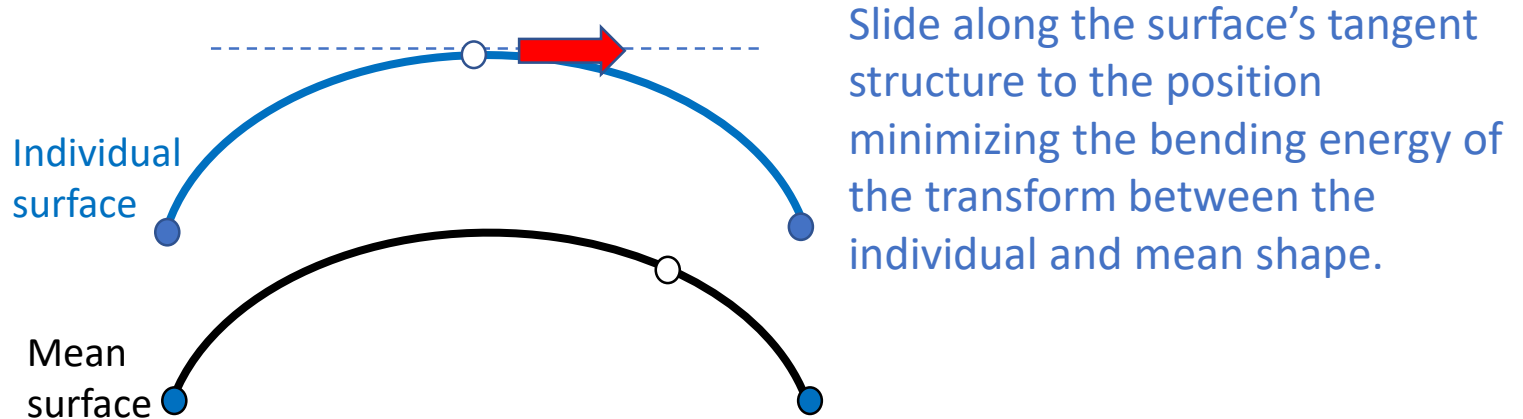


Minimum bending energy criteria

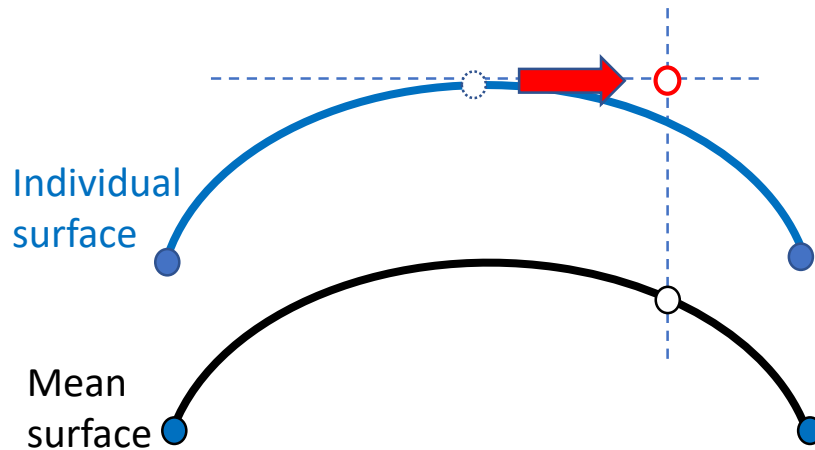


Find the line or plane tangent to the surface at the landmark point.

Minimum bending energy criteria

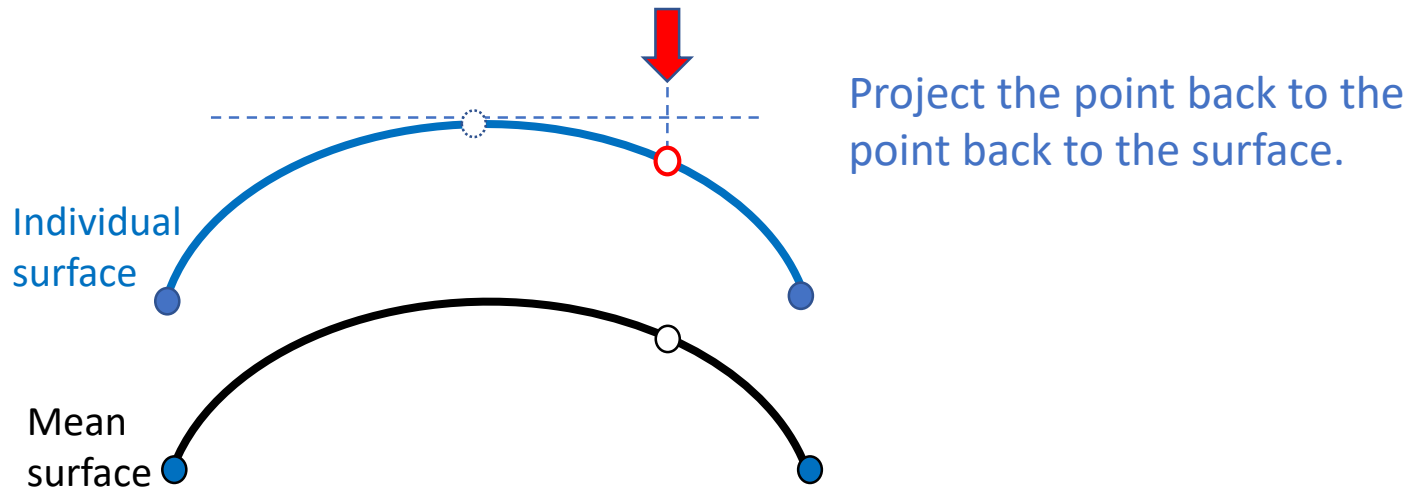


Minimum bending energy criteria

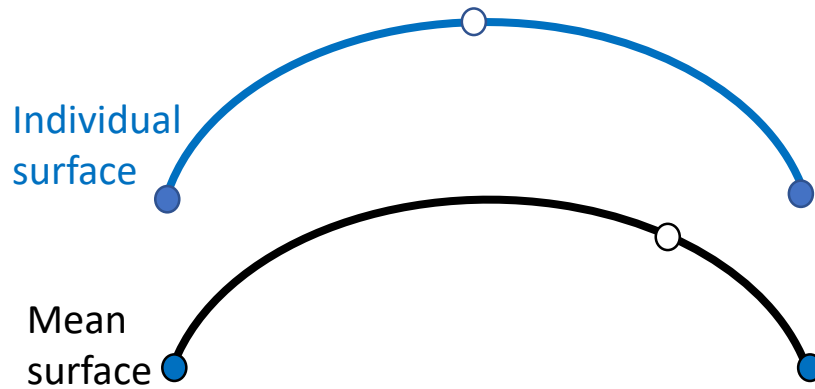


Slide along the surface's tangent structure to the position minimizing the bending energy of the transform between the individual and mean shape.

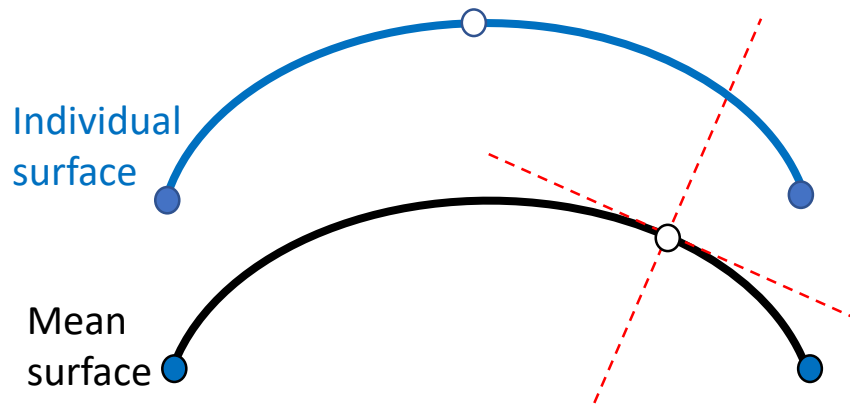
Minimum bending energy criteria



Procrustes distance criteria

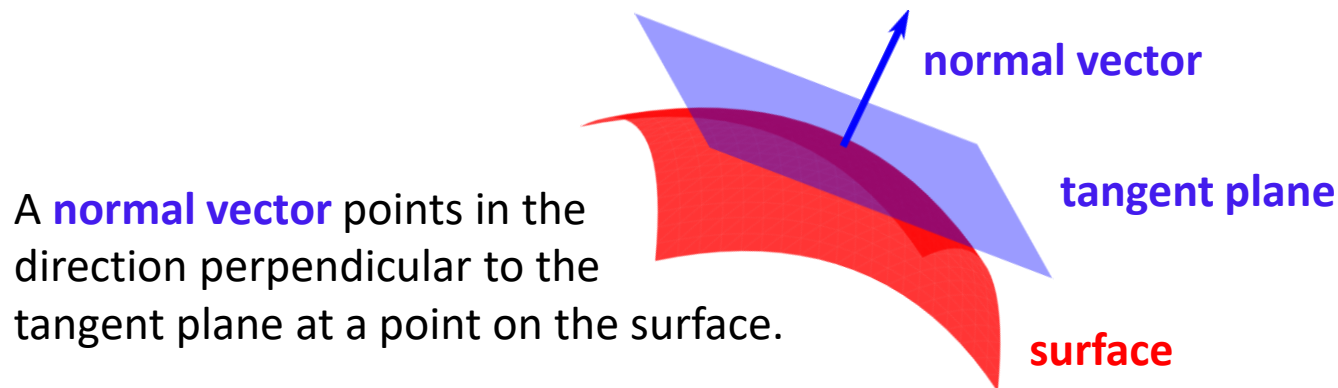
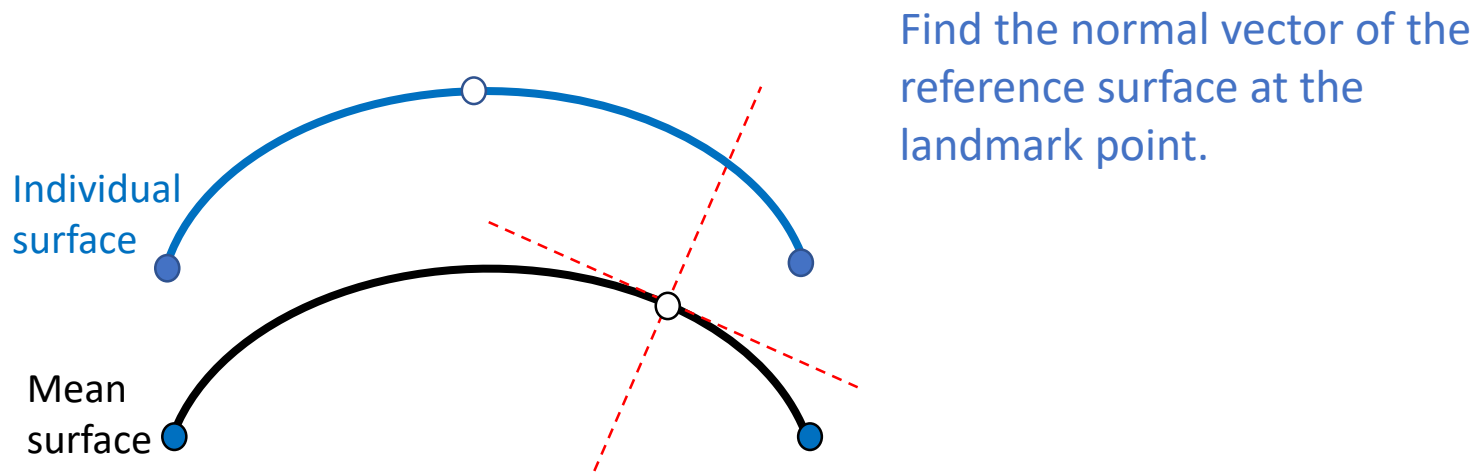


Procrustes distance criteria

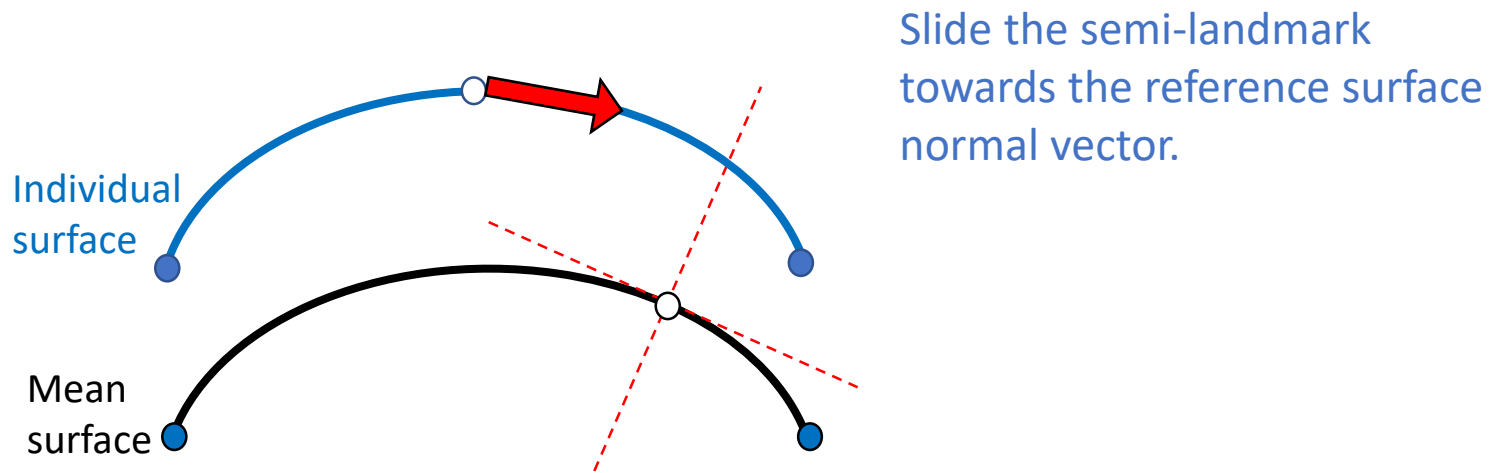


Find the normal vector of the reference surface at the landmark point.

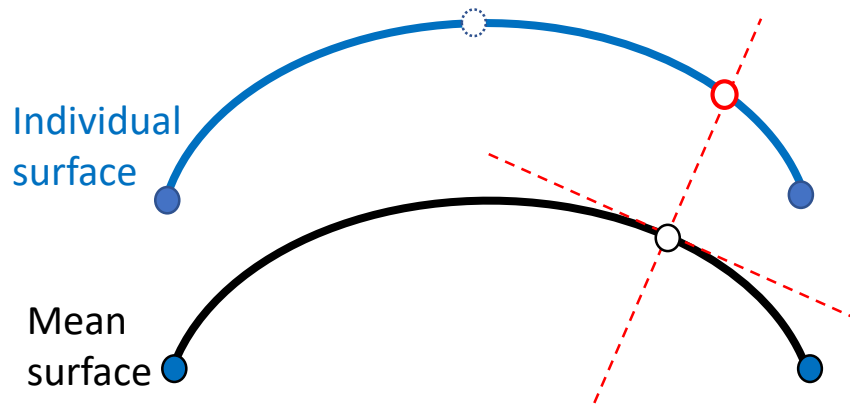
Procrustes distance criteria



Procrustes distance criteria



Procrustes distance criteria



Slide the semi-landmark
towards the reference surface
normal vector.

Minimum bending energy or Procrustes distance?

- Use different background assumptions
- The difference between the criteria can alter the results when morphological variation in the sample is low
- More noticeable with smaller numbers of semi-landmarks

Perez, S. Ivan, Valeria Bernal, and Paula N. Gonzalez. "Differences between sliding semi-landmark methods in geometric morphometrics, with an application to human craniofacial and dental variation." *Journal of anatomy* 208.6 (2006): 769-784.



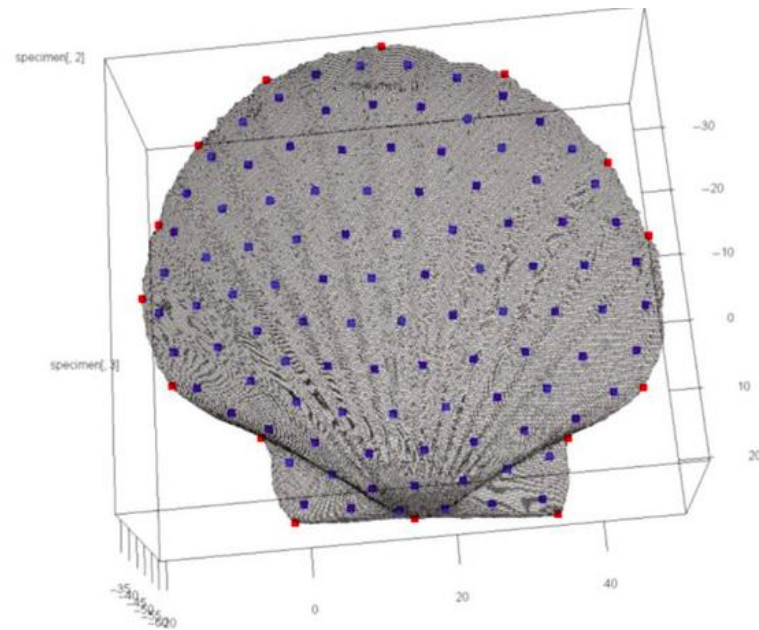
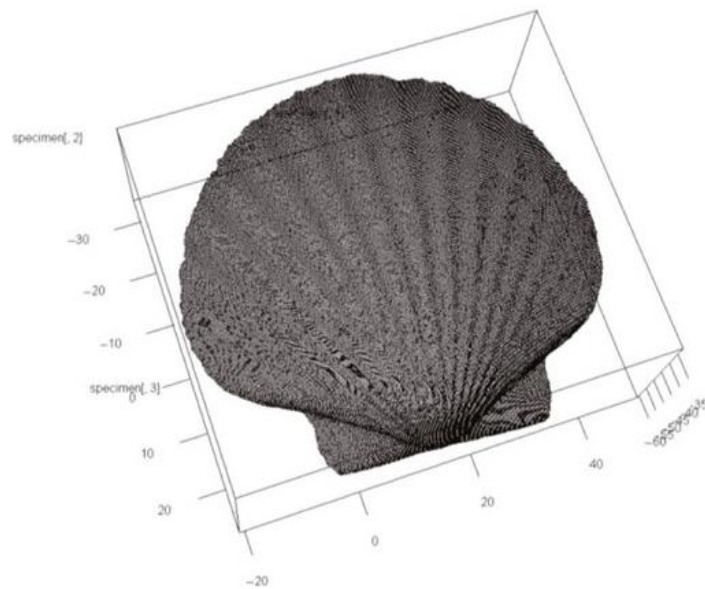
Limitations of semi-landmarks

- Limited homology
- The method of handling semi-landmarks can influence the results
- The number of semi-landmarks may also influence the results
- Semi-landmark positions are dependent on the dataset. Not possible to compare new shapes without recalculating

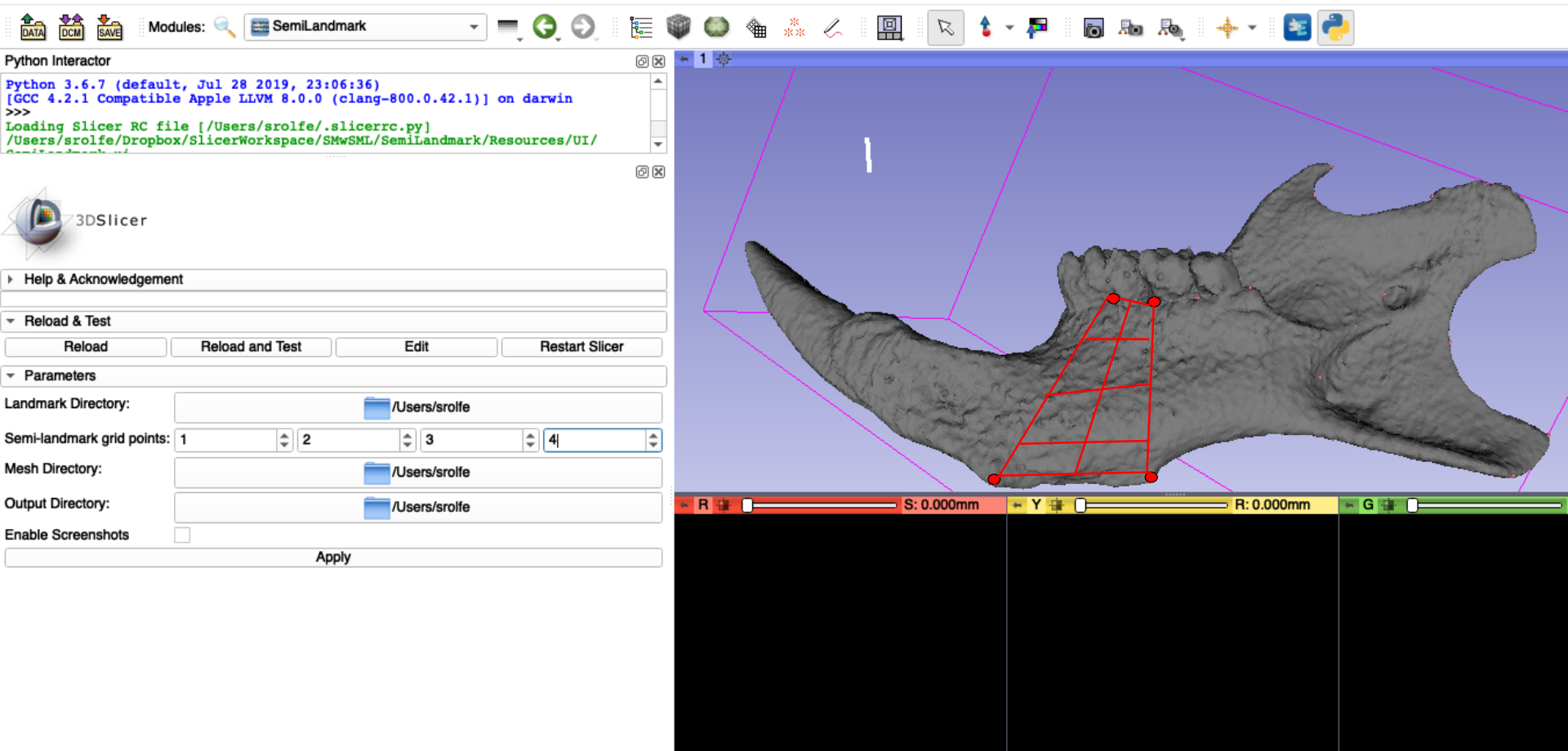


Semi-landmarks in R: Morpho

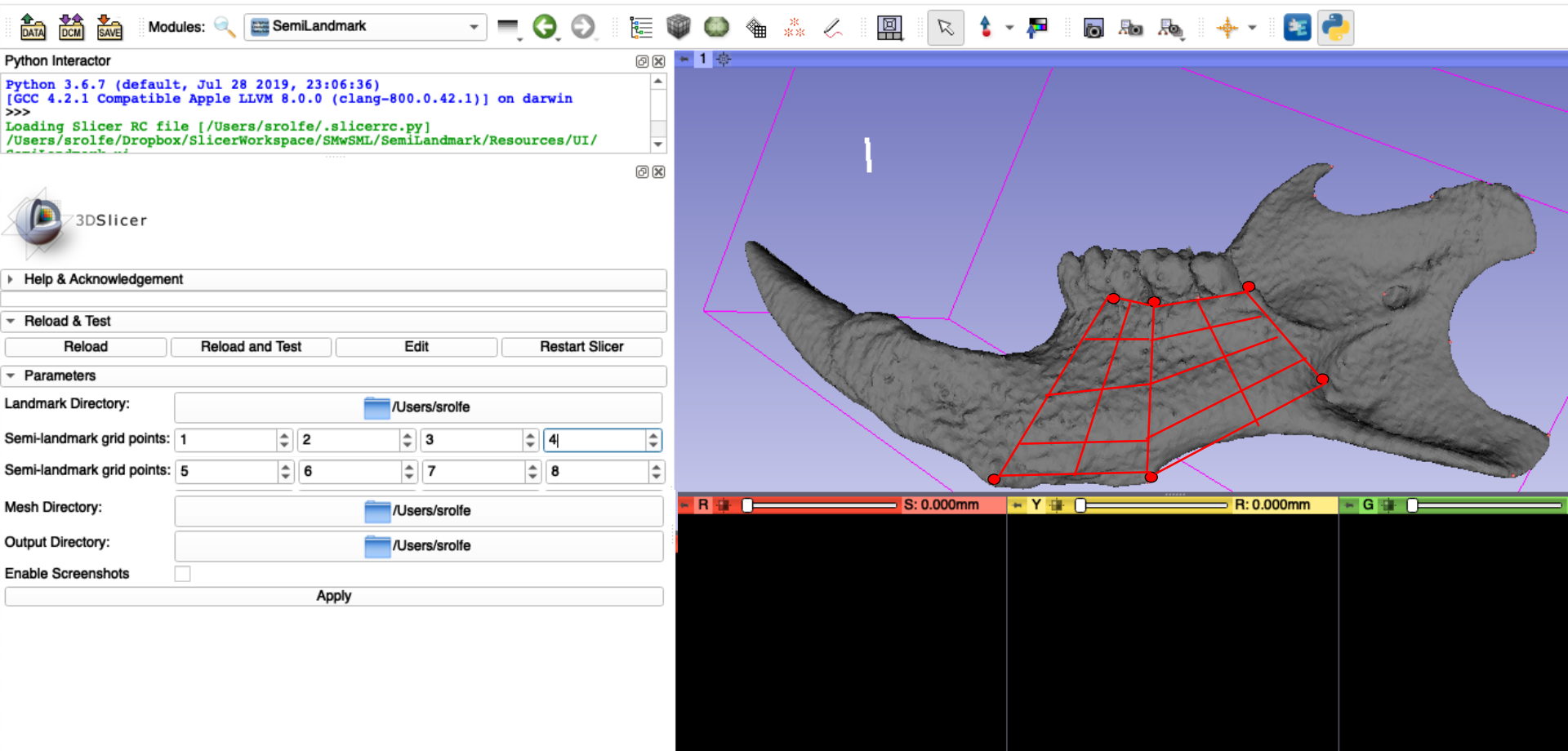
R Toolboxes [Morpho](#) and [Geomorph](#) for morphometric analysis provide support for capturing and analyzing semi-landmarks



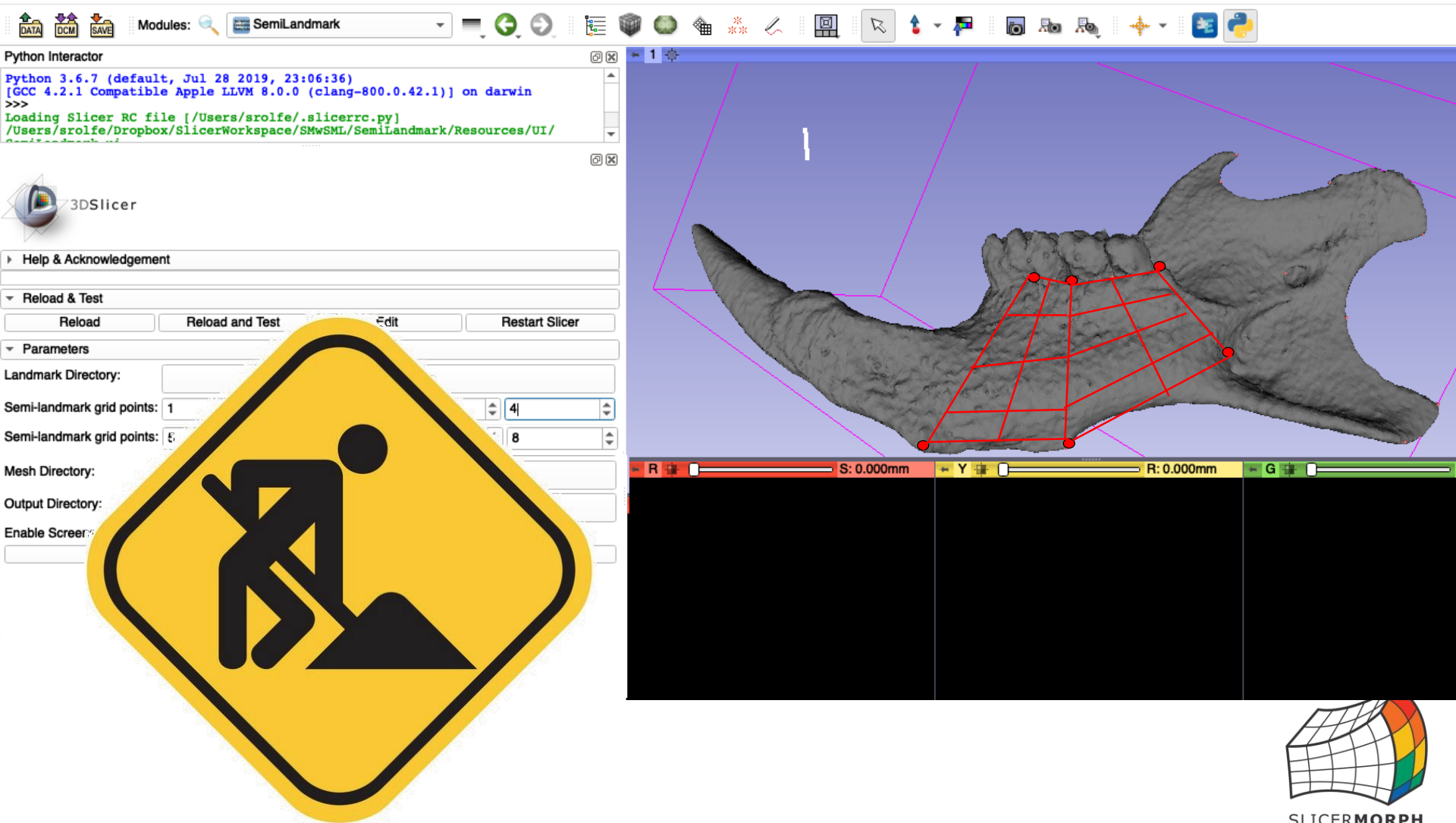
Coming soon



Coming soon

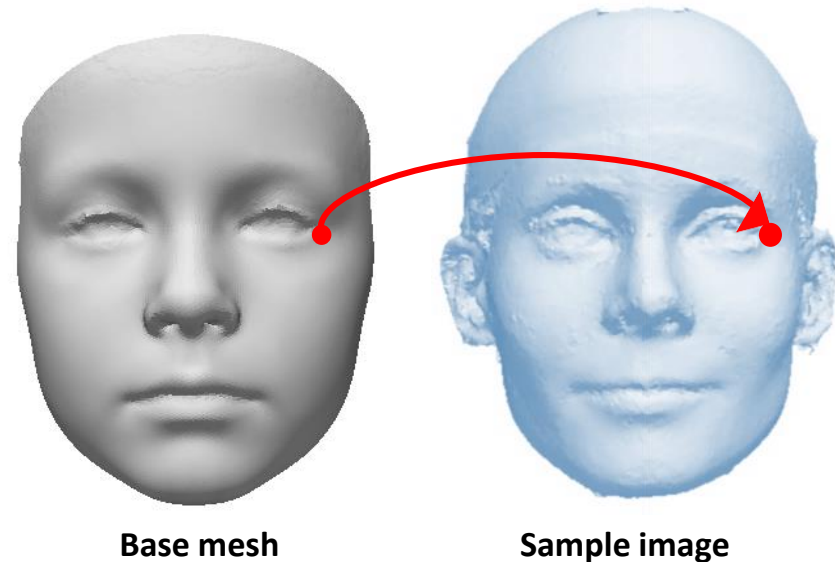


Coming soon



Deformation-based morphology (DBM)

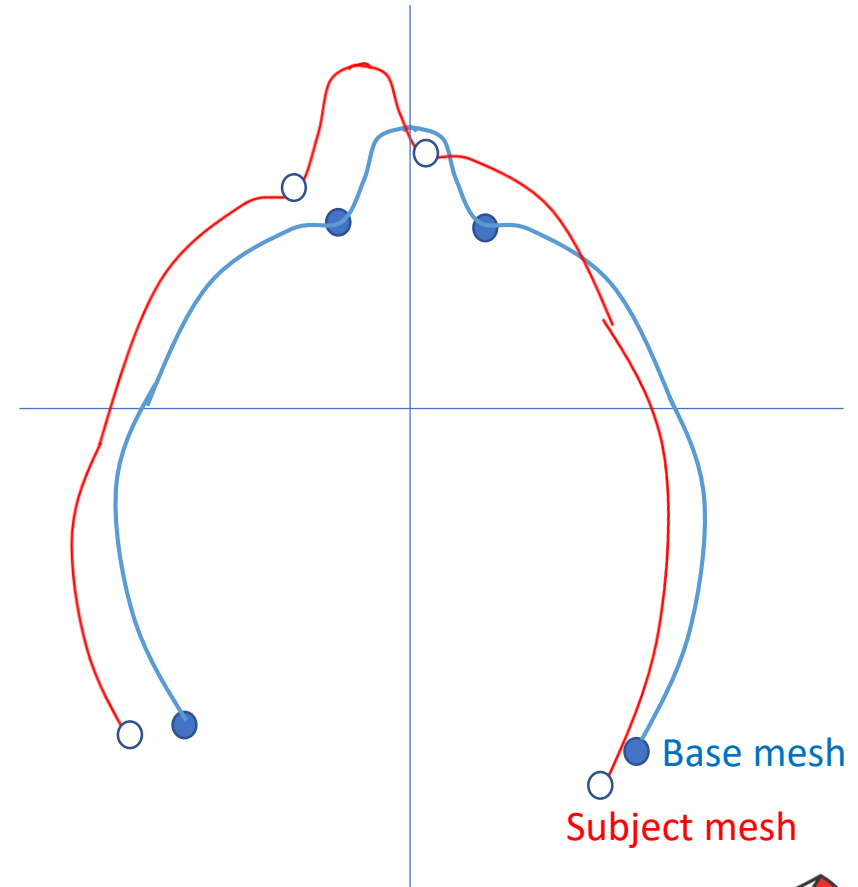
- Calculate or select a base mesh
- Establish point correspondences between the base mesh and all meshes in data set
- Vertices of the base mesh define a new set of dense surface landmarks



Hutton, T. J., Buxton, B. F., Hammond, P. (2001). "Dense surface point distribution models of the human face," in Proceedings IEEE Workshop on Mathematical Methods in Biomedical Image Analysis (MMBIA 2001) (Kauai, HI).

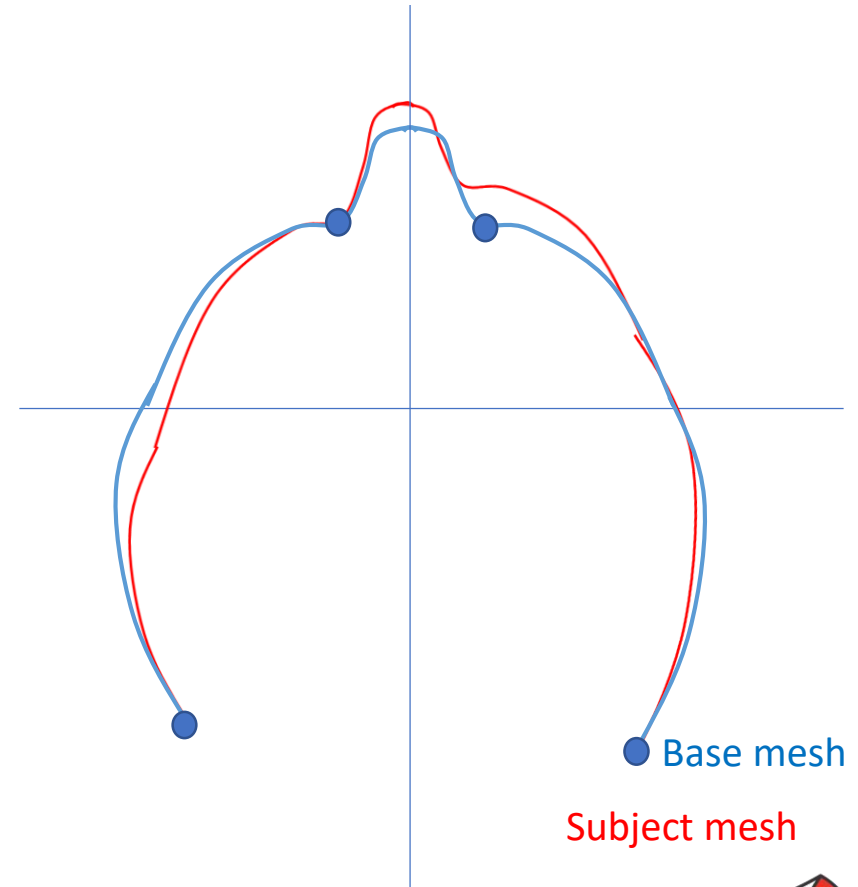


Steps to find point correspondence



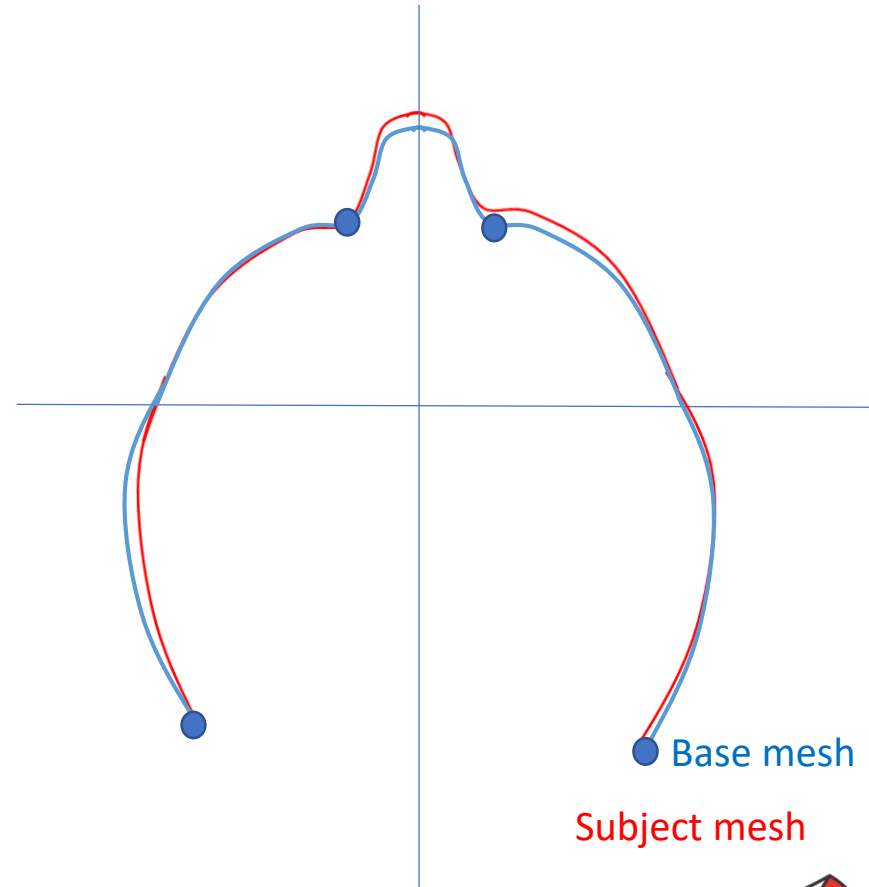
Steps to find point correspondence

1. Align anatomical landmarks with Generalized Procrustes Analysis (GPA)



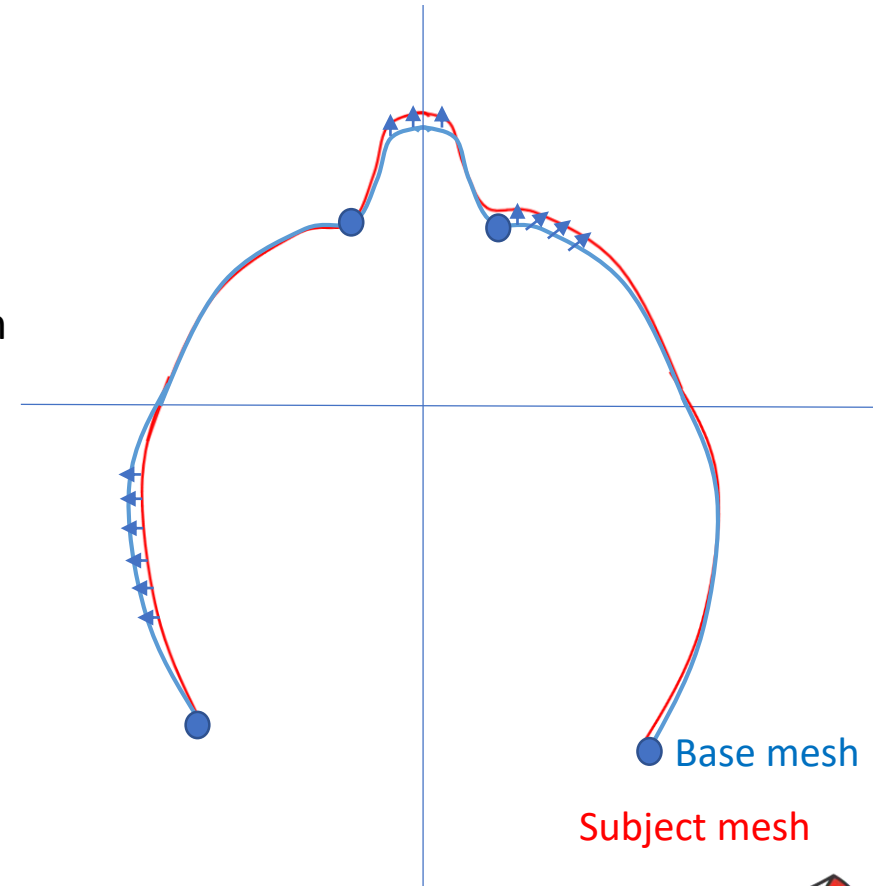
Steps to find point correspondence

1. Align anatomical landmarks with Generalized Procrustes Analysis (GPA)
2. Warp the meshes to a base mesh with a thin-plate spline (TPS) transformation



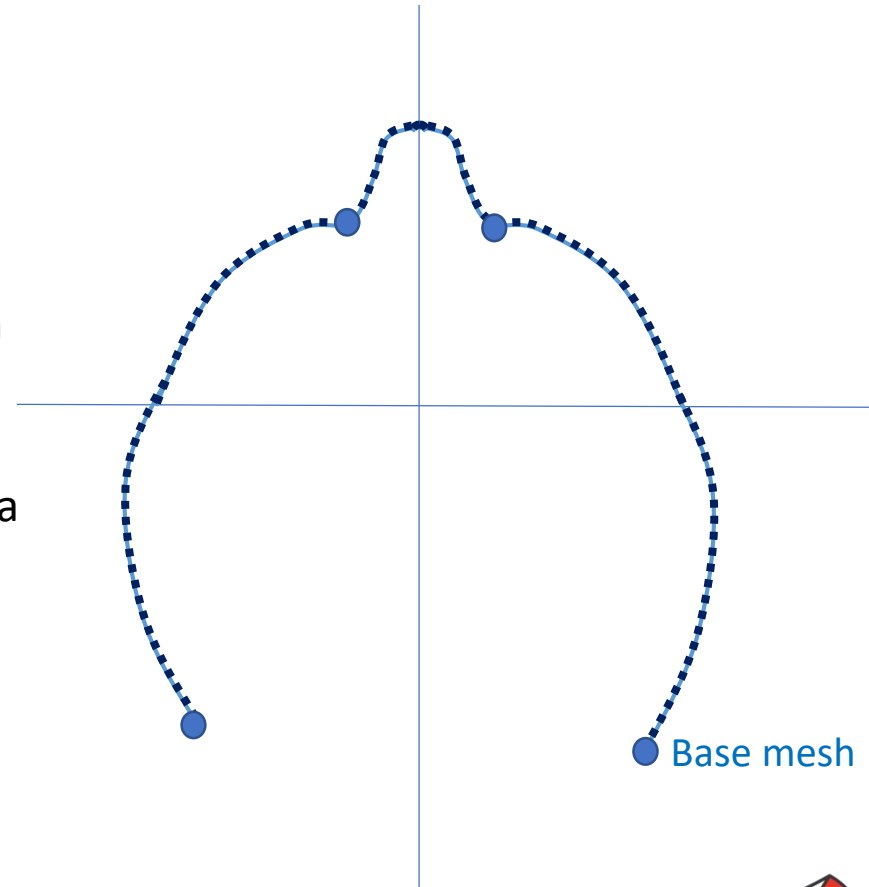
Steps to find point correspondence

1. Align anatomical landmarks with Generalized Procrustes Analysis (GPA)
2. Warp the meshes to a base mesh with a thin-plate spline (TPS) transformation
3. Determine point correspondences for each vertex the iterative closest point (ICP) algorithm



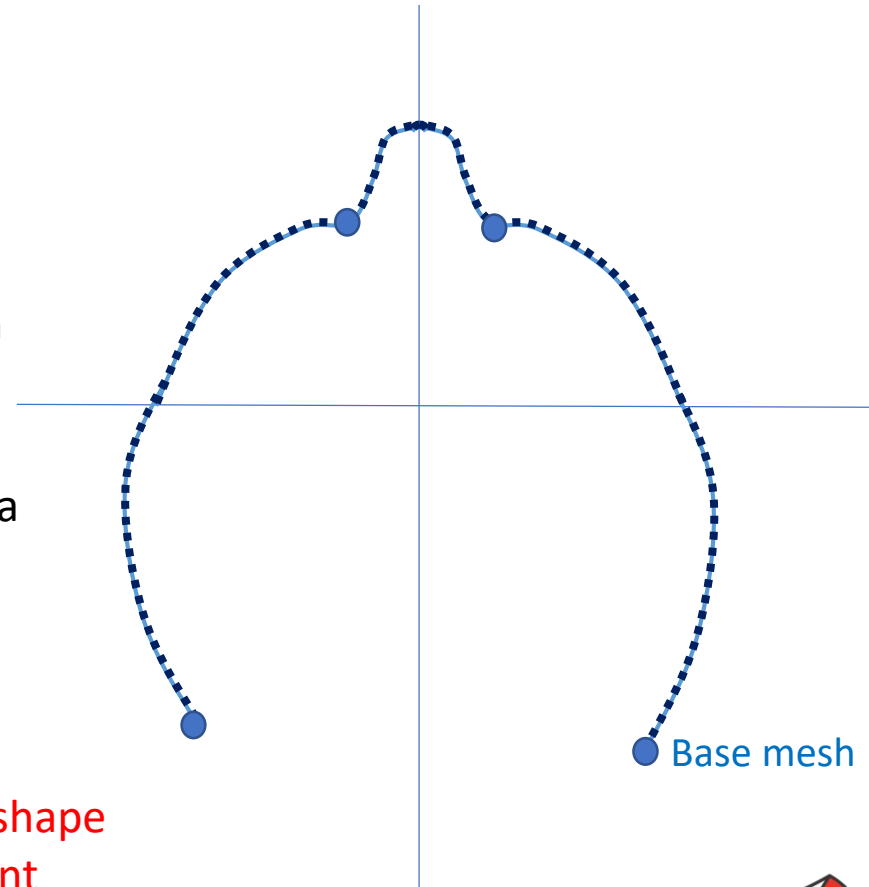
Steps to find point correspondence

1. Align anatomical landmarks with Generalized Procrustes Analysis (GPA)
2. Warp the meshes to a base mesh with a thin-plate spline (TPS) transformation
3. Determine point correspondences for each vertex the iterative closest point (ICP) algorithm
4. Each vertices of the base mesh represents a landmark point with a known correspondences for each subject



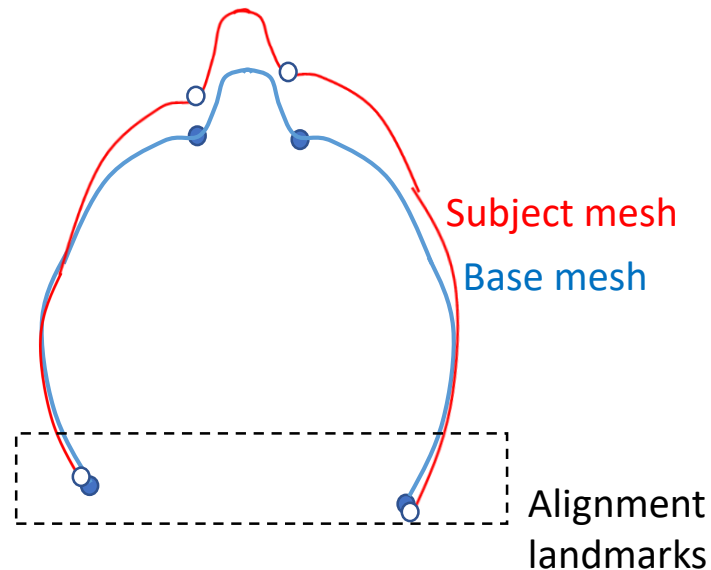
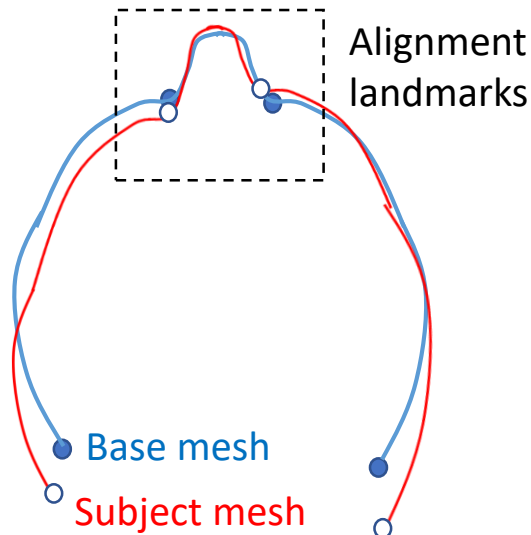
Steps to find point correspondence

1. Align anatomical landmarks with Generalized Procrustes Analysis (GPA)
 2. Warp the meshes to a base mesh with a thin-plate spline (TPS) transformation
 3. Determine point correspondences for each vertex the iterative closest point (ICP) algorithm
 4. Each vertices of the base mesh represents a landmark point with a known correspondences for each subject
- The TPS warped subjects need to be a reasonable approximation of the mean shape
 - This depends on the number of alignment landmarks and the variation in the data set

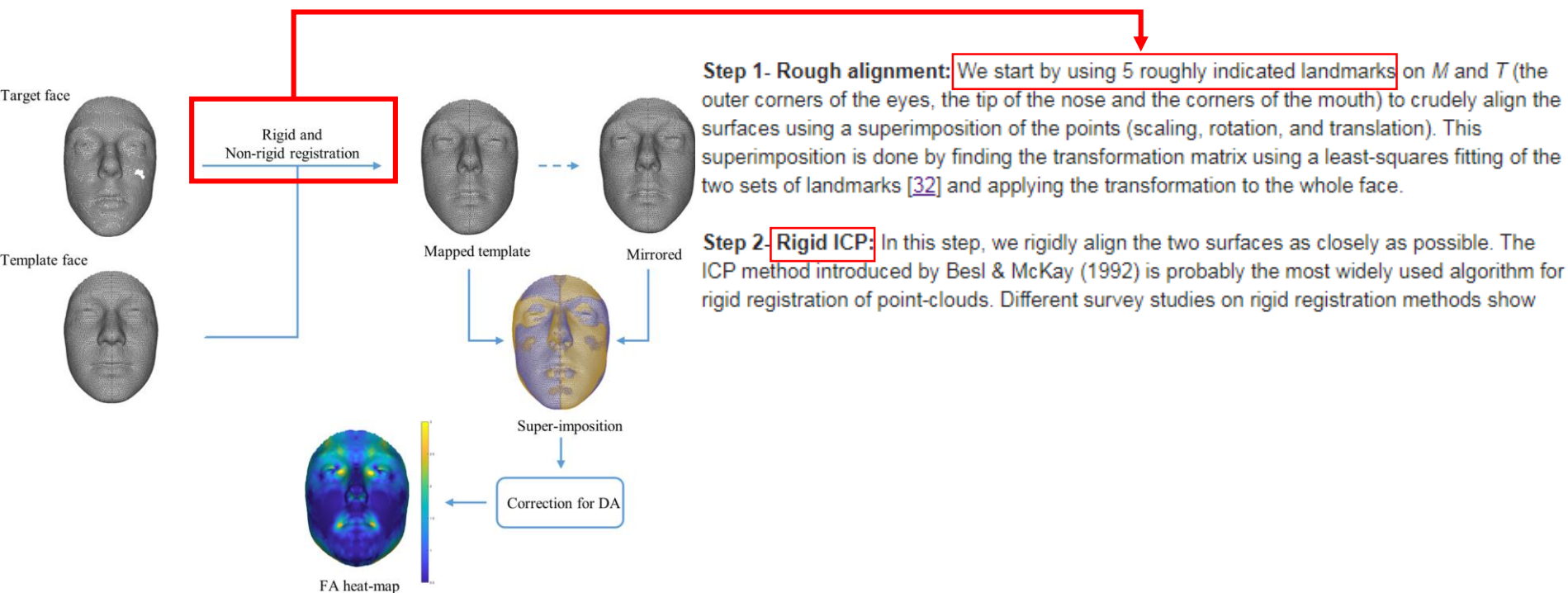


DBM is not “landmark-free”

- Initial alignment defines the frame of reference
- Choice of landmarks for alignment will impact the interpretation of the results
- Alignment landmarks with known homology will provide an interpretable framework for shape change measured

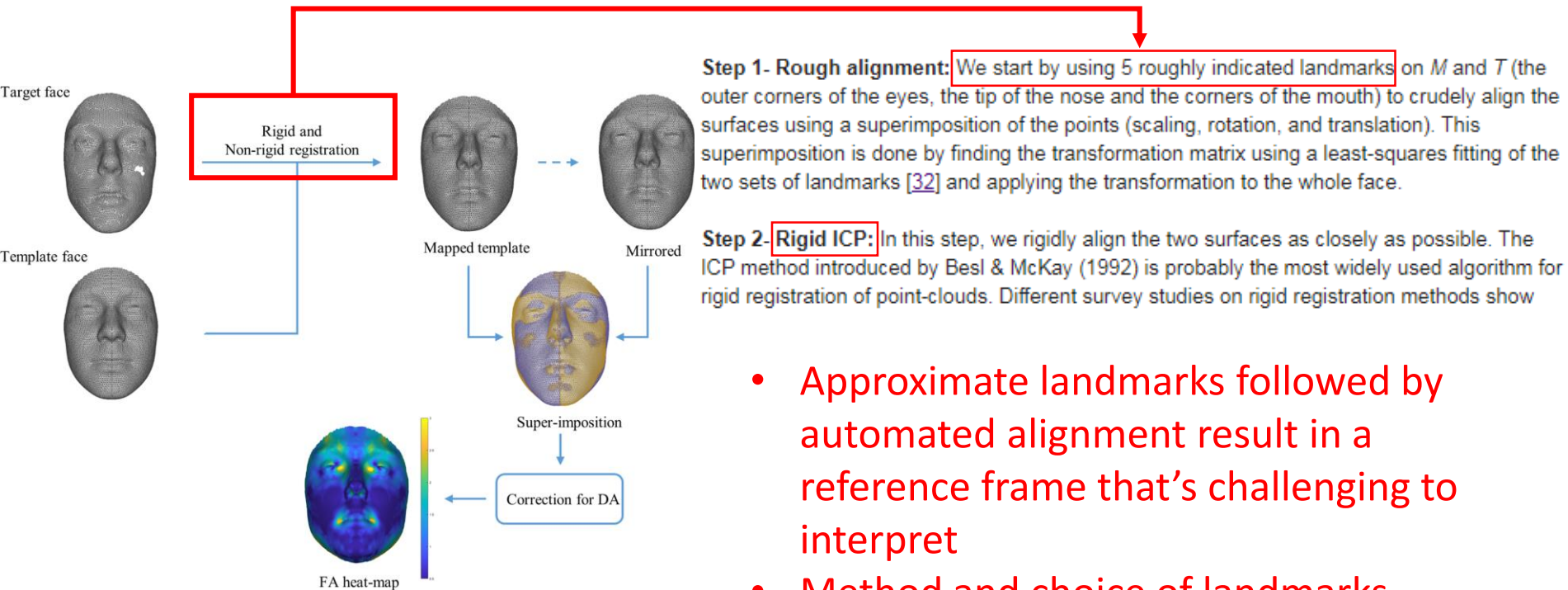


Initial alignment in DBM



Ekrami, Omid, et al. "Measuring asymmetry from high-density 3D surface scans: An application to human faces." *PloS one* 13.12 (2018): e0207895.

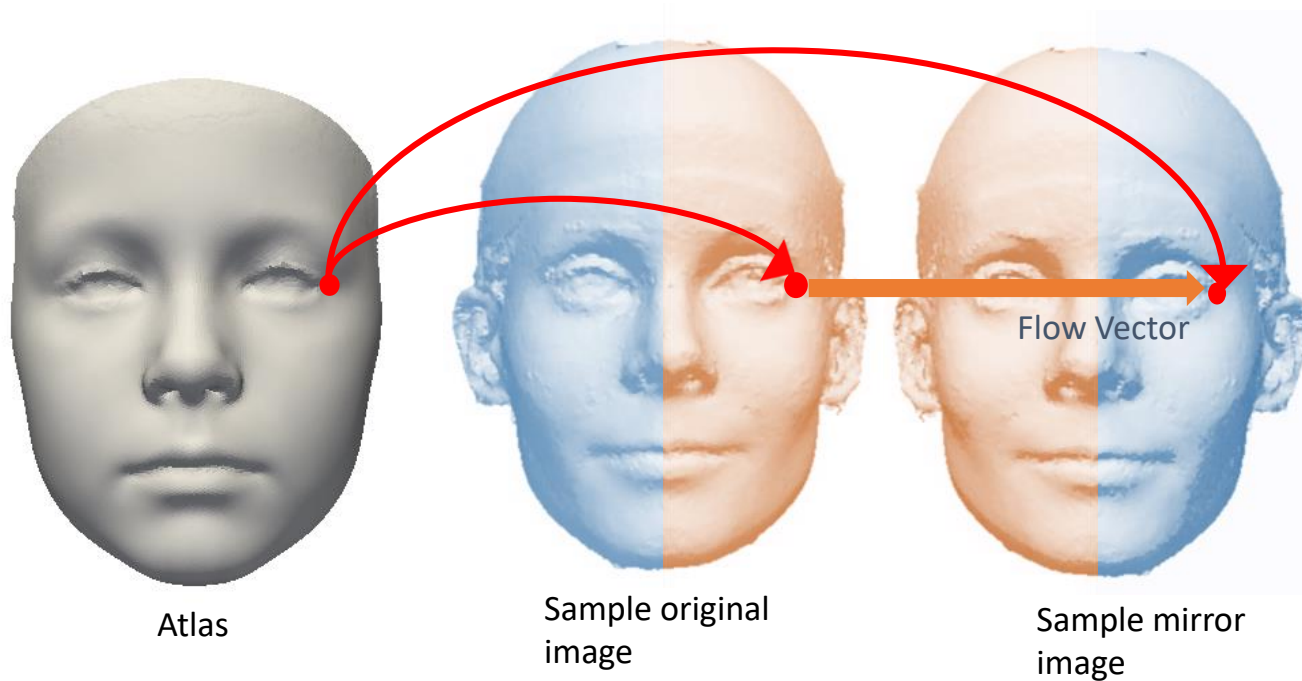
Initial alignment in DBM



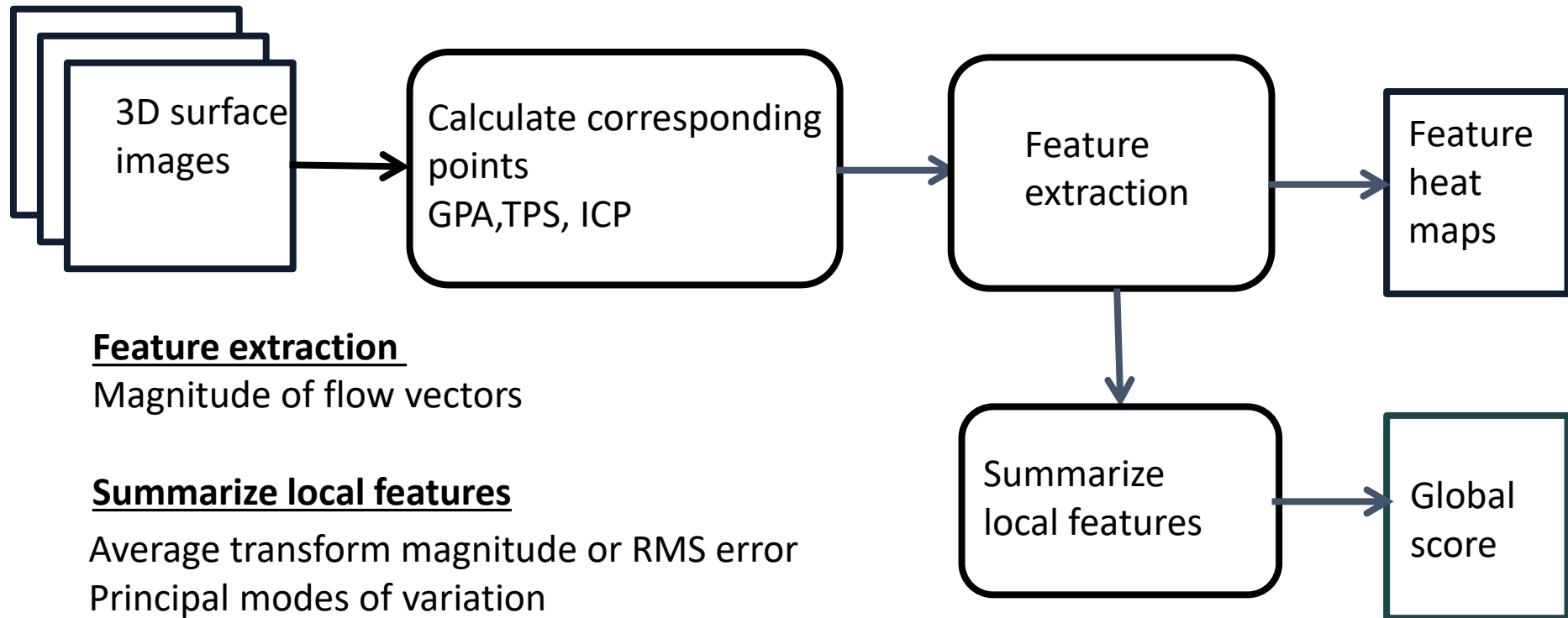
- Approximate landmarks followed by automated alignment result in a reference frame that's challenging to interpret
- Method and choice of landmarks should be carefully evaluated

Ekrami, Omid, et al. "Measuring asymmetry from high-density 3D surface scans: An application to human faces." *PloS one* 13.12 (2018): e0207895.

Dense model of facial asymmetry



Quantifying facial asymmetry with Dense Surface Models



Feature extraction

Magnitude of flow vectors

Summarize local features

Average transform magnitude or RMS error

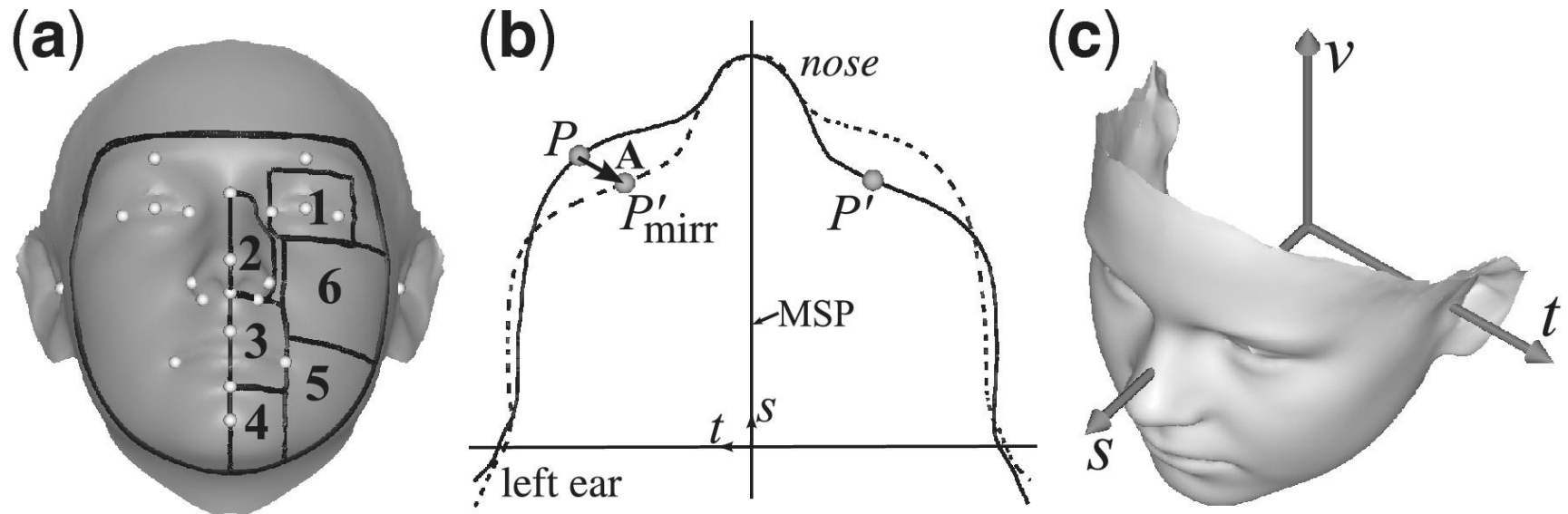
Principal modes of variation

Facial signatures (Hammond et al., 2012)

BRIM method (Claes et al., 2014)

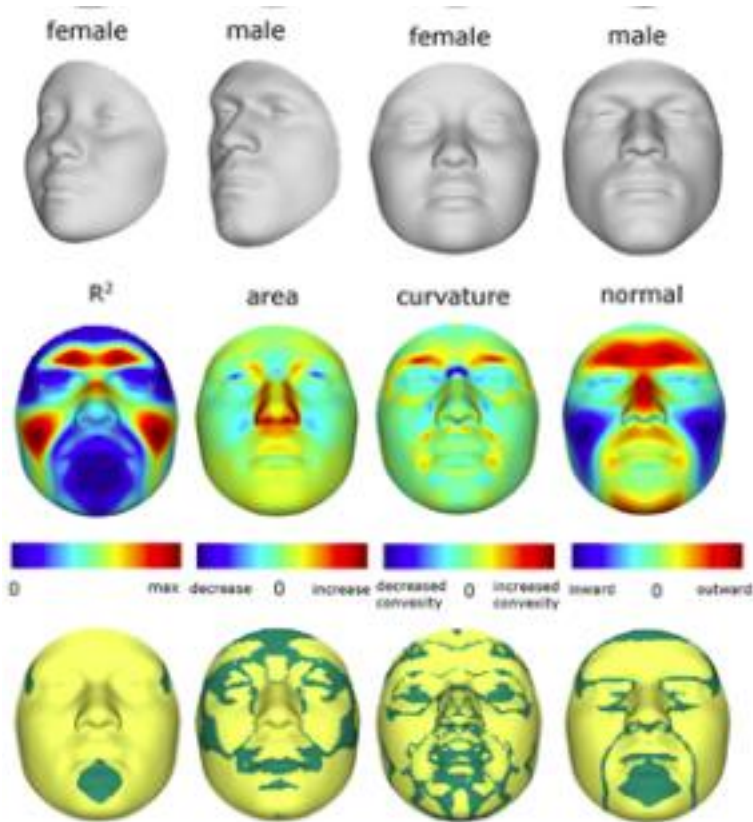


Automated Quantification of facial asymmetry



Darvann, Tron A., et al. "Automated quantification and analysis of facial asymmetry in children with arthritis in the temporomandibular joint." *2011 IEEE International Symposium on Biomedical Imaging: From Nano to Macro*. IEEE, 2011.

BRIM: bootstrapped response-based imputation modeling



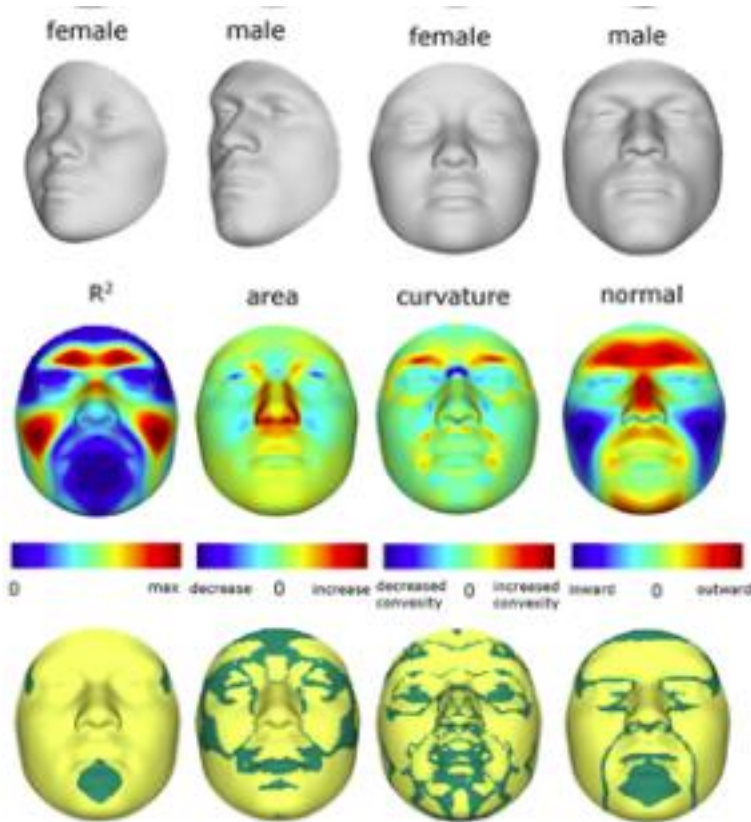
- Technique to investigate the genetic basis for variation in the shape of the human face
- Estimation of a single quantitative axis of variation correspond to effects of single genes, ancestry, or sex

Claes, Peter, et al. "Modeling 3D facial shape from DNA." *PLoS genetics* 10.3 (2014): e1004224.

Hallgrímsson, Benedikt, et al. "Let's face it—complex traits are just not that simple." *PLoS genetics* 10.11 (2014): e1004724.



BRIM: bootstrapped response-based imputation modeling



- Technique to investigate the genetic basis for variation in the shape of the human face
- Estimation of a single quantitative axis of variation correspond to effects of single genes, ancestry, or sex

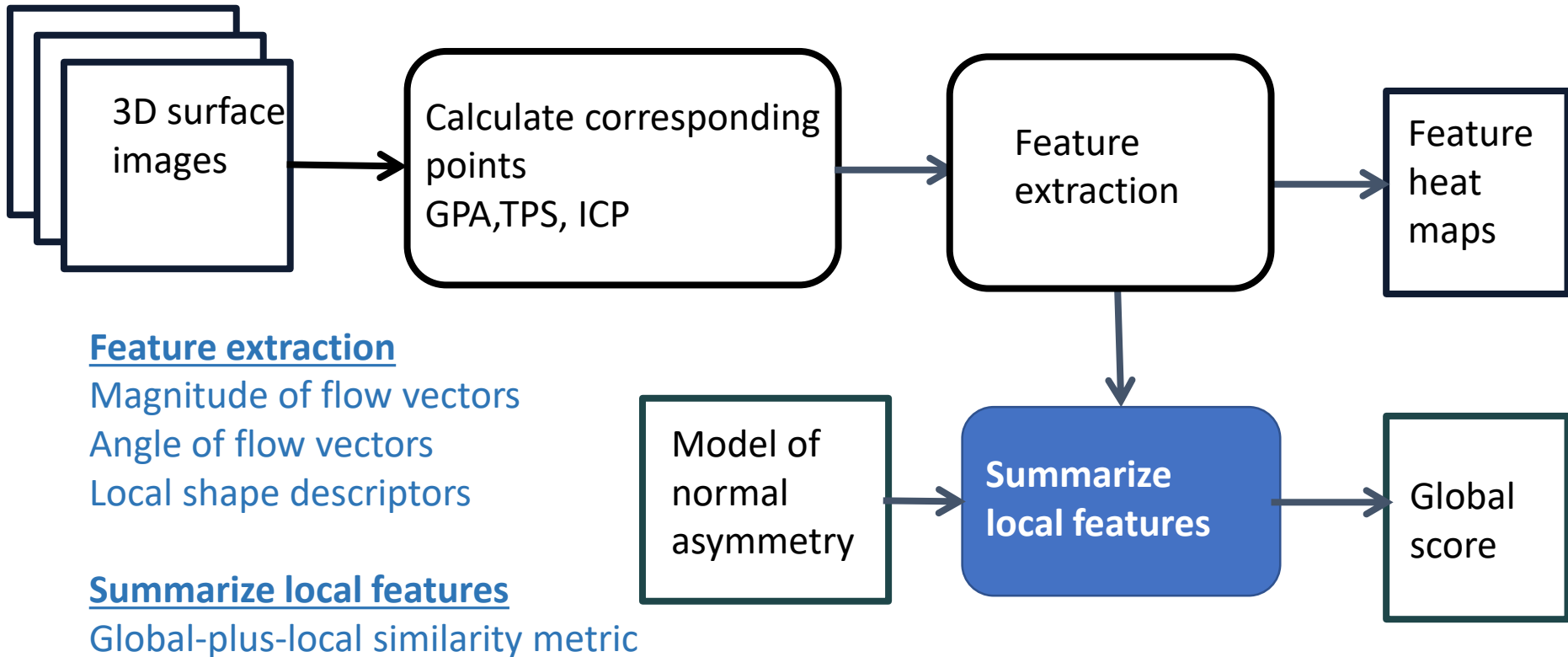
“...our methods provide the means of identifying the genes that affect facial shape and for modeling the effects of these genes to generate a predicted face.”

Claes, Peter, et al. "Modeling 3D facial shape from DNA." *PLoS genetics* 10.3 (2014): e1004224.

Hallgrímsson, Benedikt, et al. "Let's face it—complex traits are just not that simple." *PLoS genetics* 10.11 (2014): e1004724.

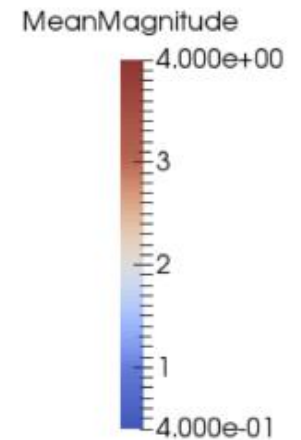
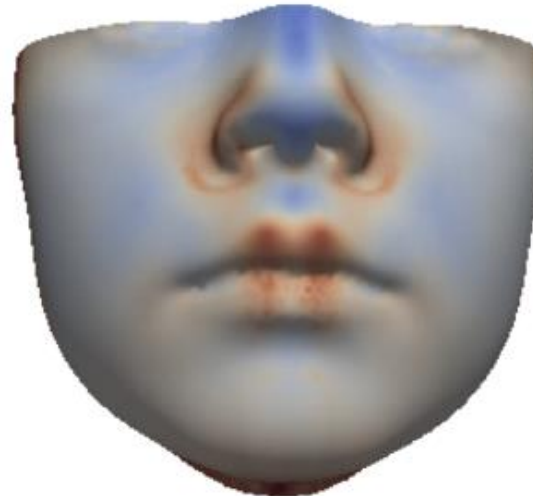


Summarizing local features

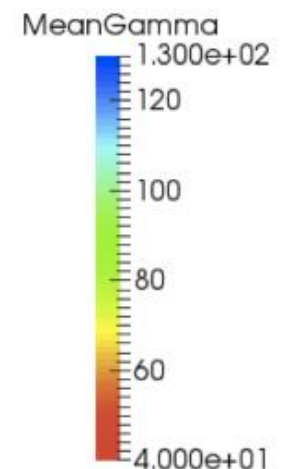
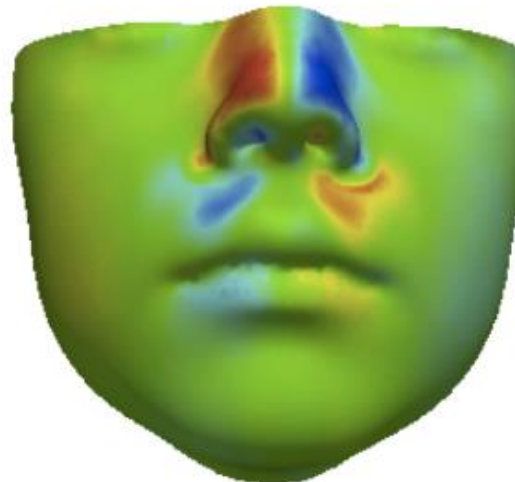


Feature Heat Maps

Magnitude Feature



Angle of deformation

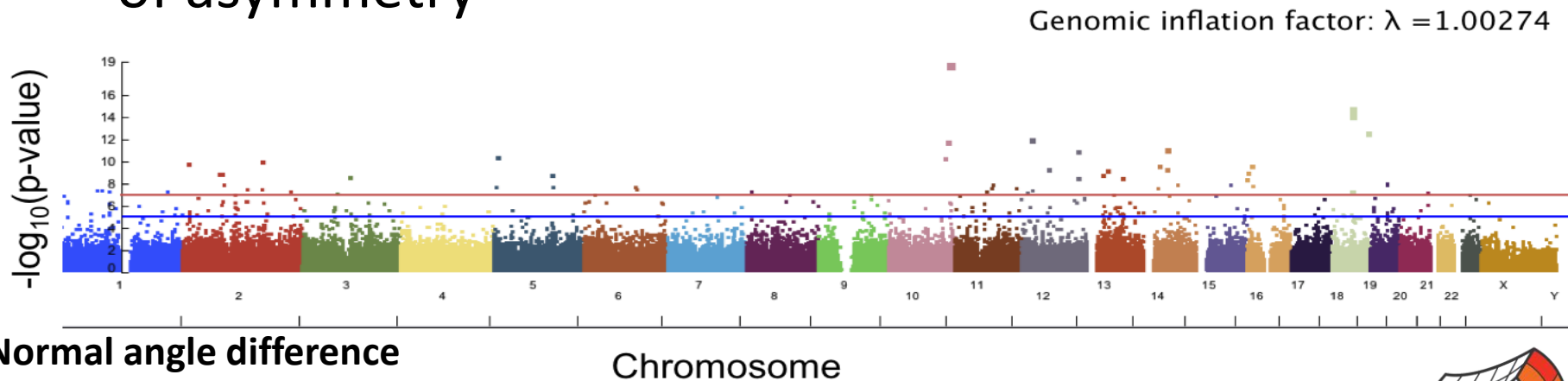


Average of normal asymmetry

Abnormal Asymmetry

Genetic basis of facial asymmetry

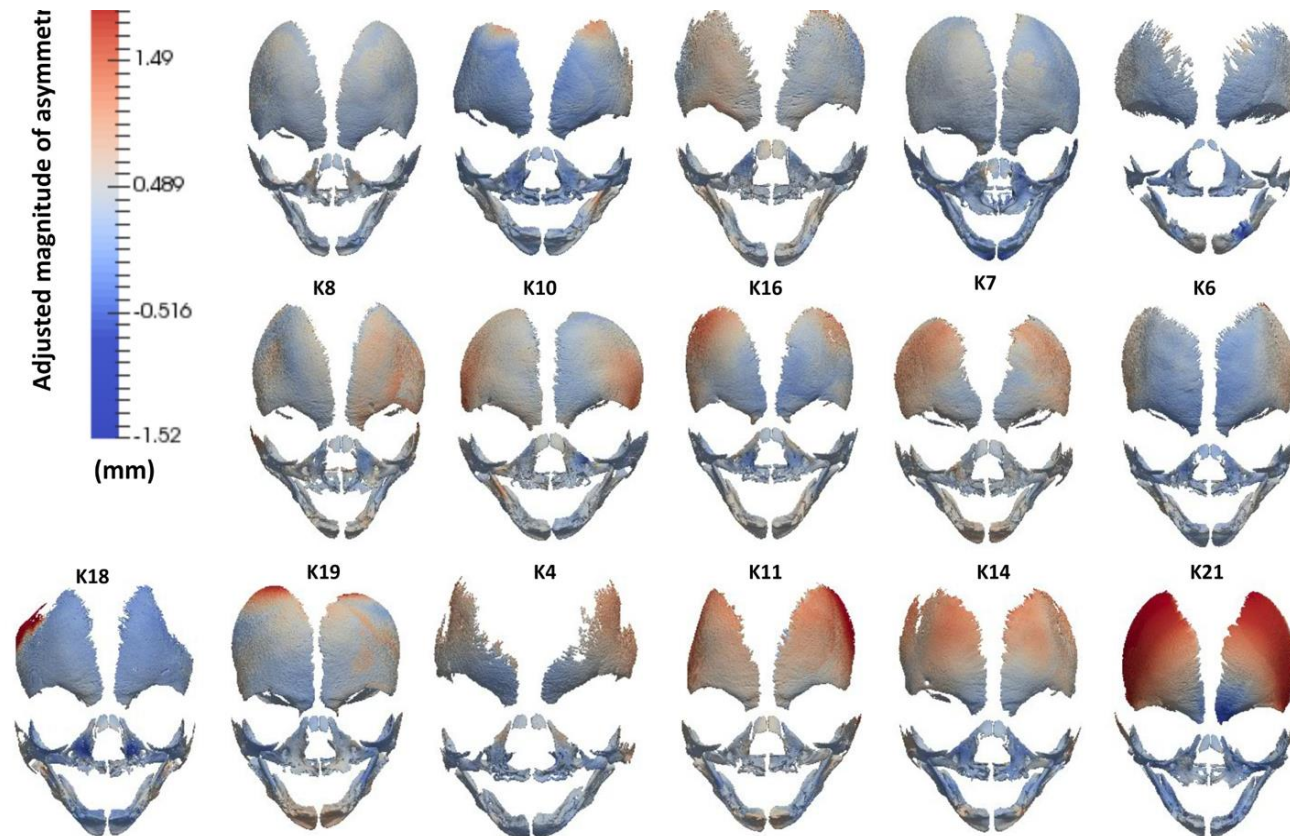
- Aim to use automated phenotyping to produce a score of facial asymmetry that can summarize local deviations from normal asymmetry
- Correlate with SNP data to investigate genetic basis of asymmetry



Rolfe, Sara, Su-In Lee, and Linda Shapiro. "Associations between genetic data and quantitative assessment of normal facial asymmetry." *Frontiers in genetics* 9 (2018): 659.



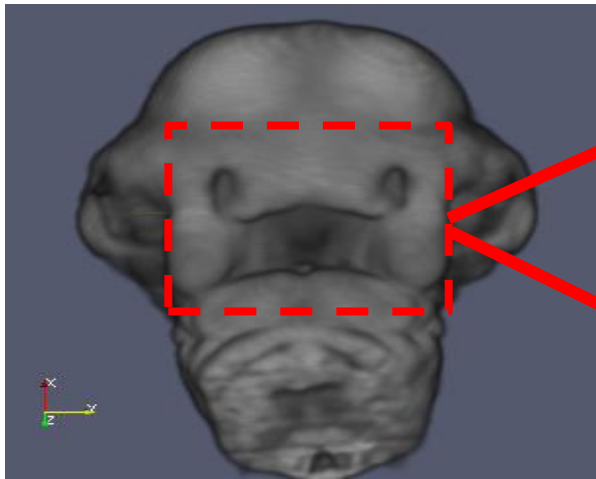
Analysis of asymmetry in developing facial bones



Katsube, M., Rolfe, S.M., Bortolussi, S.R., Yamaguchi, Y., Richman, J.M., Yamada, S. and Vora, S.R., 2019. Analysis of facial skeletal asymmetry during foetal development using μ CT imaging. *Orthodontics & craniofacial research*, 22, pp.199-206.

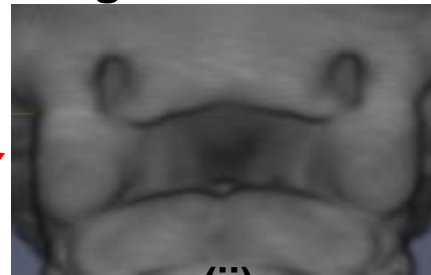
Feature Heat Maps

Normal Reference Image

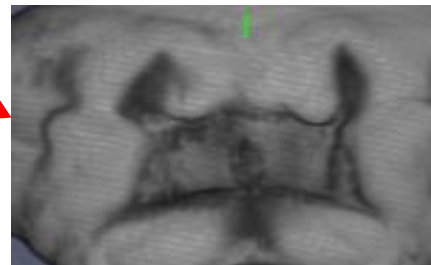


(i)

Zoom of Facial Region

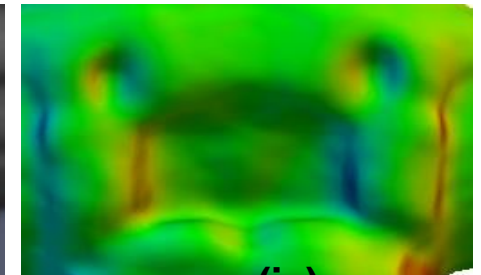


(ii)

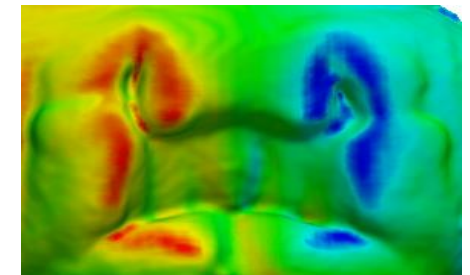


(iii)

Angle Heat Map



(iv)

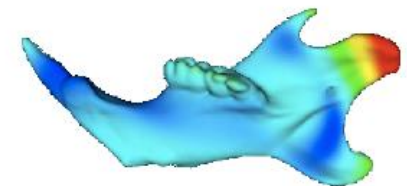
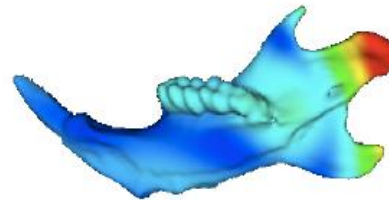
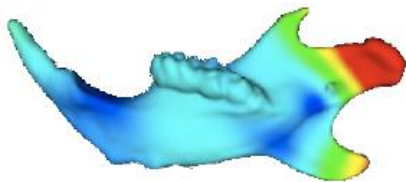


(v)

Retrieval of Specimen with Similar Morphological Shape Differences

Magnitude Sample Query

Magnitude
Heat Map



Left/Right
Overlay



(i) Query Image

(ii) First Result

(iii) Second Result

Correlation between distance from most asymmetric and expert asymmetry ranking = 0.91

Rolfe, S. M., Camci, E. D., Mercan, E., Shapiro, L. G., & Cox, T. C. "A New Tool for Quantifying and Characterizing Asymmetry in Bilaterally Paired Structures." IEEE EMBS '13 Jul 2013.

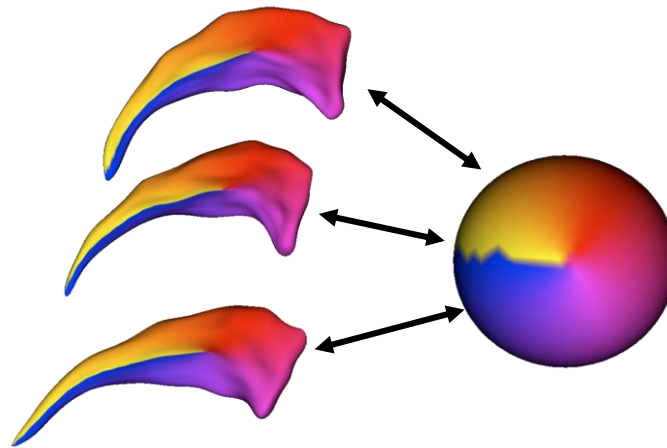
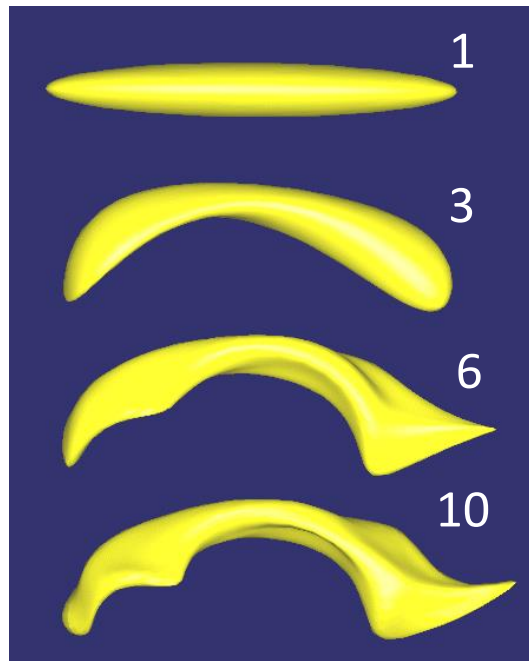


Limitations of DBM

- No guarantee of homology
- Results need to be interpreted with respect to initial alignment
- High dimensional data output
- Computationally intensive for large datasets



Spherical harmonic representation and point distributed models (SPHARM-PDM)

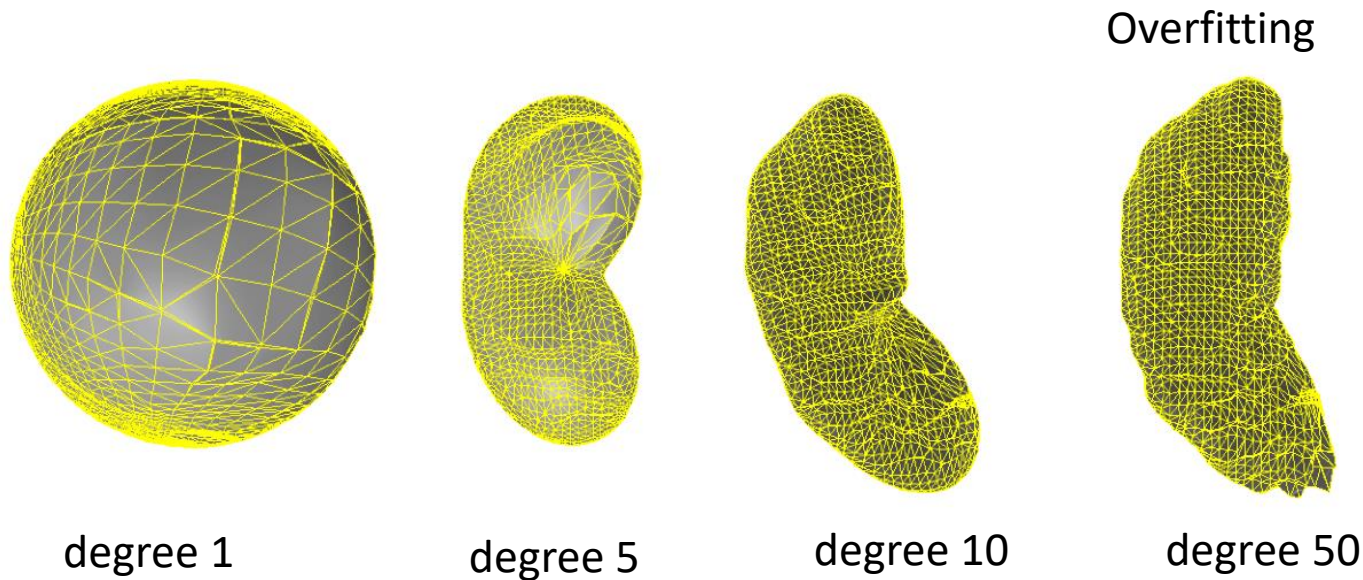


SPHARM
description is
computed from
the mesh and its
spherical
parameterization

Styner, Lieberman, Pantazis, Gerig: Boundary and Medial Shape Analysis of the Hippocampus in Schizophrenia, Medical Image Analysis, 2004, pp 197-203

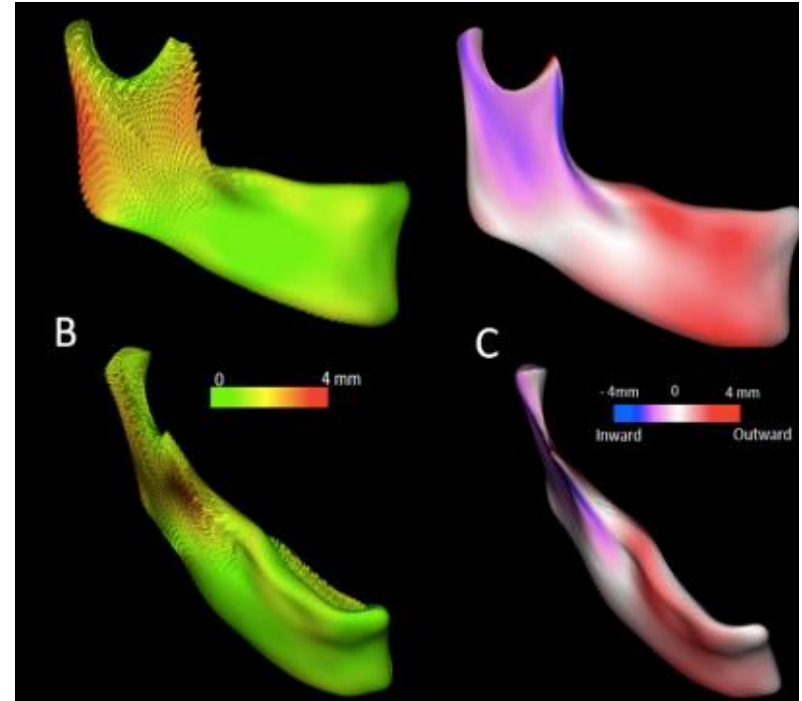
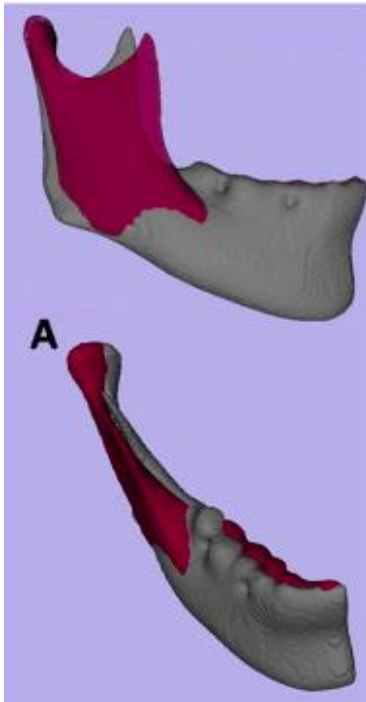


SPHARM modeling



- The SPHARM description is then sampled into a triangulated surface
- Triangulated surfaces with correspondences are computed via icosahedron of the spherical parameterization

SPHARM analysis of mandibular asymmetry



Cevitanes, Lucia HS, et al. "Three-dimensional quantification of mandibular asymmetry through cone-beam computerized tomography." *Oral Surgery, Oral Medicine, Oral Pathology, Oral Radiology, and Endodontology* 111.6 (2011): 757-770.

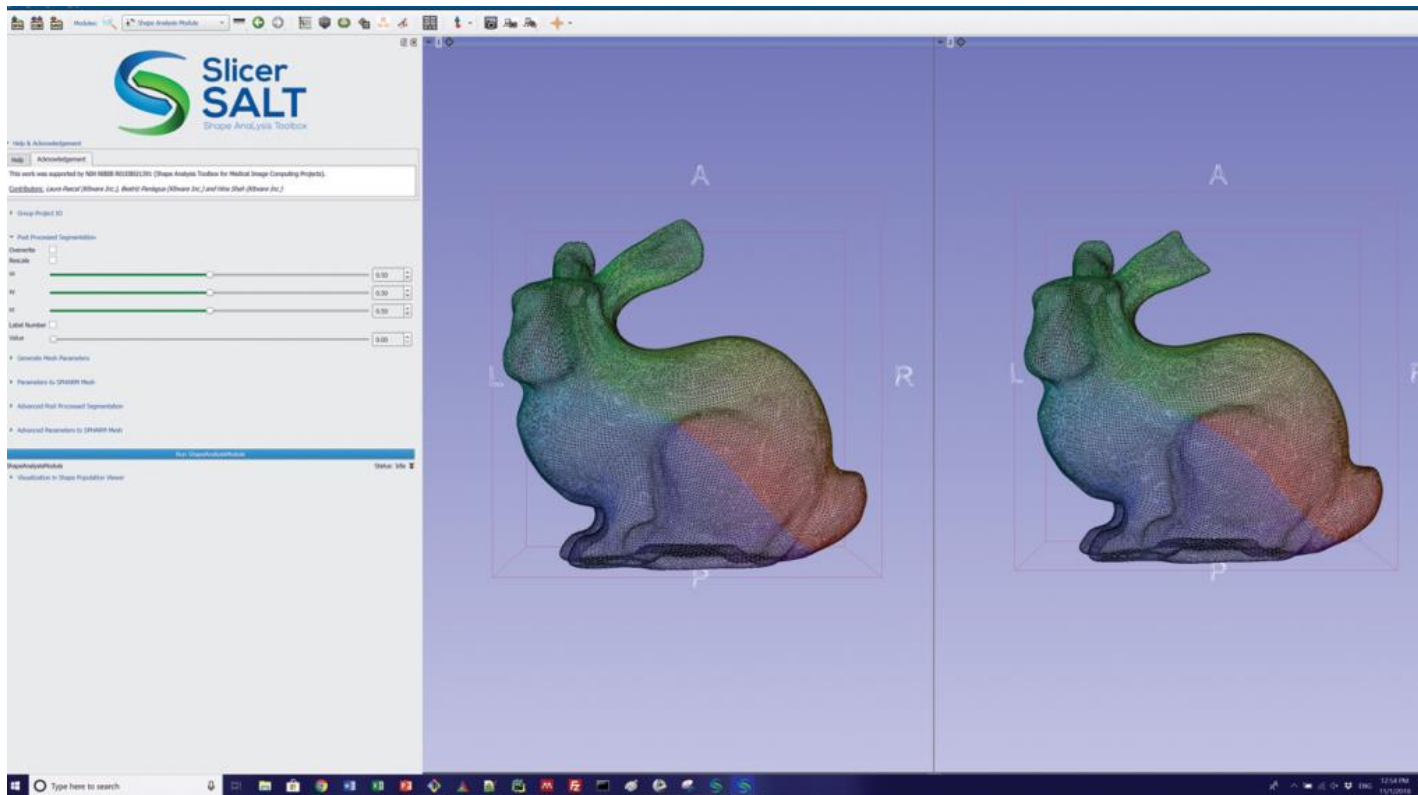


Limitations of SPHARM methods

- Requirement for spherical topology of meshes
- Challenging for complicated or noisy data sets
- Developed for high N of shapes with similar morphology – should preform a quality assessment to check for correspondence issues



Slicer SALT: Shape AnaLysis Toolbox

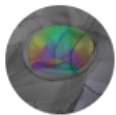


Compute point
distributed
models (pdm)
using spherical
harmonic
representation
(SPHARM-PDM)



Coming soon

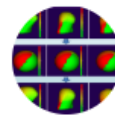
With SlicerSALT you can...



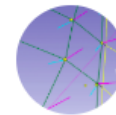
Compute Point Distributed Models (PDM) using Spherical Harmonic Representation (SPHARM-PDM)



Run 4D regression in a collection of 3D PDMs associated to a linear variable (i.e. age)



Perform correspondence optimization using study-wise shape analysis



Fit skeletal representations (s-reps) to a collection of binary volumes



Compute image-based correspondence in binary volumes of non-spherical and complex topologies



Use advanced shape statistics for scientific hypothesis testing



Access all functionality through the graphical user interface



Perform command line batch processing



SLICERMORPH

Questions?



Resources

Watanabe, Akinobu. "How many landmarks are enough to characterize shape and size variation?." *PloS one* 13.6 (2018): e0198341.

Moyers, Robert E., and Fred L. Bookstein. "The inappropriateness of conventional cephalometrics." *American Journal of Orthodontics and Dentofacial Orthopedics* 75.6 (1979): 599-617.

Bookstein, Fred L., and William DK Green. "A feature space for edgels in images with landmarks." *Journal of Mathematical imaging and vision* 3.3 (1993): 231-261.

Cutting, Court, et al. "A three-dimensional smooth surface analysis of untreated Crouzon's syndrome in the adult." *The Journal of craniofacial surgery* 6.6 (1995): 444-453.

Andresen, Per Rønsholt, and Mads Nielsen. "Non-rigid registration by geometry-constrained diffusion." *Medical Image Analysis* 5.2 (2001): 81-88.

Gunz, Philipp, Philipp Mitteroecker, and Fred L. Bookstein. "Semilandmarks in three dimensions." *Modern morphometrics in physical anthropology*. Springer, Boston, MA, 2005. 73-98.

Perez, S. Ivan, Valeria Bernal, and Paula N. Gonzalez. "Differences between sliding semi-landmark methods in geometric morphometrics, with an application to human craniofacial and dental variation." *Journal of anatomy* 208.6 (2006): 769-784.

Ekrami, Omid, et al. "Measuring asymmetry from high-density 3D surface scans: An application to human faces." *PloS one* 13.12 (2018): e0207895.

Darvann, Tron A., et al. "Automated quantification and analysis of facial asymmetry in children with arthritis in the temporomandibular joint." *2011 IEEE International Symposium on Biomedical Imaging: From Nano to Macro*. IEEE, 2011.

Styner, Lieberman, Pantazis, Gerig: Boundary and Medial Shape Analysis of the Hippocampus in Schizophrenia, *Medical Image Analysis*, 2004, pp 197-203

